

Oskarshamn site investigation

$^{40}\text{Ar}/^{39}\text{Ar}$ dating of fracture minerals

Henrik Drake, Earth Sciences Centre, Göteborg University

Laurence Page, Department of Geology, Lund University

Eva-Lena Tullborg, Terralogica AB

January 2007

Svensk Kärnbränslehantering AB
Swedish Nuclear Fuel
and Waste Management Co
Box 5864
SE-102 40 Stockholm Sweden
Tel 08-459 84 00
+46 8 459 84 00
Fax 08-661 57 19
+46 8 661 57 19



Oskarshamn site investigation

$^{40}\text{Ar}/^{39}\text{Ar}$ dating of fracture minerals

Henrik Drake, Earth Sciences Centre, Göteborg University

Laurence Page, Department of Geology, Lund University

Eva-Lena Tullborg, Terralogica AB

January 2007

Keywords: Simpevarp, Laxemar, Äspö, fracture minerals, Geochronology, Adularia, Illite, Muscovite, Apophyllite, Hornblende.

This report concerns a study which was conducted for SKB. The conclusions and viewpoints presented in the report are those of the authors and do not necessarily coincide with those of the client.

A pdf version of this document can be downloaded from www.skb.se

Abstract

This report presents the results obtained from geochronological studies of fracture minerals from the Laxemar and Simpevarp subareas and Äspö. Thirteen drill core samples of K-bearing minerals (adularia, muscovite, apophyllite, illite and hornblende) from both open and sealed fractures have been dated with the $^{40}\text{Ar}/^{39}\text{Ar}$ method. The samples are from drill cores from the cored boreholes KA1755A (Äspö), KSH01A and KSH03A+B (Simpevarp) and KLX02, KLX03, KLX06 and KLX08 (Laxemar).

Fracture minerals have been selected to provide absolute geochronological constraints of the relative sequence of fracture mineralizations obtained by e.g. cross-cutting relations and stable isotope analyses /Drake and Tullborg 2004, 2005, 2006ab, 2007/. The sequence consists of seven generations of which generation 1 and 6 have been dated in the present study. Furthermore, greisen-like fillings (thought to be coeval with generation 3 and 4) and muscovite in altered wall rock (related to generation 3 and 4) have also been dated in the present study.

The analyses yielded plateau ages for ten samples. Seven samples yielded reasonable ages (adularia and muscovite) in accordance with interpretations from cross-cutting relations, chemistry and isotope studies /Drake and Tullborg 2004, 2005, 2006ab, 2007/, while two samples yielded younger ages than expected (adularia and muscovite). Four samples did not yield plateau ages or gave insignificant ages (illite, apophyllite and hornblende).

Reliable ages were obtained for generation 3 and 4 (wall rock muscovite; $1,417 \pm 3$ Ma) and for the greisen related fracture fillings in KLX06 ($1,423 \pm 3$ Ma, $1,424 \pm 2$ Ma and $1,424 \pm 2$ Ma) which shows that these fracture fillings as well as the major part of the red-staining of the wall rock in the area are related to the intrusion of the Götemar granite (and probably also Uthammar granite).

The Palaeozoic generation (6) of fracture fillings was also successfully dated by obtained ages of 401, 426 and 443–448 Ma, which is in accordance with earlier datings of this generation in the Götemar granite /Sundblad et al. 2004/. This generation is related in time with the Caledonian orogeny and the development of its foreland basin.

Ductile shear zones in the area are thought to predate the intrusions at Götemar and Uthammar (~ 1,440–1,450 Ma). The age obtained for muscovite in a mylonite of generation 1 (1,406 Ma) is, thus, younger than the presumed mylonite formation. The obtained age is thought to represent either re-activation of the mylonites (and formation of muscovite) during the intrusions of the Götemar and Uthammar granites or resetting of the Ar-system in the muscovite due to thermal affect during the emplacement of these intrusions. A K-feldspar of generation 3 gave a Sveconorwegian age (989 Ma) which is younger than expected. It can either be a generation 3 K-feldspar that has been reset during the Sveconorwegian orogeny or that the K-feldspar actually was formed during Sveconorwegian reactivation.

Sammanfattning

I denna rapport presenteras resultat från geokronologiska studier av sprickmineral från borrkärnor från Oskarshamns platsundersökning. Tretton borrkärneprover med kaliummineral (adular, muskovit, illit, apofyllit och hornblände), från både öppna och läkta sprickor, har daterats med hjälp av $^{40}\text{Ar}/^{39}\text{Ar}$ -metoden. Proverna är från borrkärnorna KA1755A (Äspö), KSH01A och KSH03A+B (Simpevarp) samt KLX02, KLX03, KLX06 och KLX08 (Laxemar).

Sprickmineral har valts ut för att ge absolut geokronologisk data till den relativa sekvensen av sprickmineraliseringar som är baserad på bl.a. klippande relationer och stabila isotoper /Drake and Tullborg 2004, 2005, 2006ab, 2007/. Sekvensen består av sju olika sprickmineralgeneratörer varav generation 1 och 6 har daterats i denna studie. Greisen-liknande fyllningar (troligen likåldriga med generation 3 and 4) och muskovit från sidoberget relaterad till generation 3 and 4 har också daterats i denna studie.

Analyserna gav platå-åldrar för tio prover. Sju prover gav förväntade åldrar (adular och muskovit) medan två prover gav lägre åldrar än förväntat (adular och muskovit). Fyra prover gav inga platå-åldrar eller irrelevanta åldrar. De förväntade åldrarna överensstämmer med tidigare tolkningar baserade på klippande relationer, kemi och isotopstudier etc. /Drake and Tullborg 2004, 2005, 2006ab, 2007/.

Tillförlitliga åldrar gavs för generation 3 och 4 (muskovit i omvandlat sidoberg; $1\,417 \pm 3$ Ma) och för de greisenliknande sprickorna i KLX06 ($1\,423 \pm 3$ Ma, $1\,424 \pm 2$ Ma och $1\,424 \pm 2$ Ma), vilket visar att dessa sprickor och även huvuddelen av den utbredda rödfärgningen runt sprickor i området är relaterade till Götemargranitens (och troligen även Uthammargranitens) intrusion.

Den Palaeoziska generationen (6) gav också tillförlitliga åldrar på 401, 426 och 443–448 Ma, vilket stämmer överens med tidigare dateringar av denna generation i Götemargraniten /Sundblad et al. 2004/. Tidsmässigt är denna generation relaterad till den Kaledoniska orogenesen och troligen också utvecklingen av en förlandsbassäng.

Myloniterna i området tros vara äldre än intrusionerna av Götemar- och Uthammargraniterna (~ 1 440–1 450 Ma). Åldern av muskovit från en mylonit tillhörande generation 1 (1 406 Ma) antas därför inte representera mylonitbildningen. Istället tros denna ålder representera en reaktivering av myloniterna (och bildning av muskovit) i samband med intrusionerna av Götemar- och Uthammargraniterna eller att Ar-systemet i den daterade muskoviten nollställts i samband med dessa intrusioner. En kalifältspat som tros tillhöra generation 3 gav en svekonorvegisk ålder (989 Ma). Denna ålder är yngre än förväntat och kan antingen bero på att kalifältspaten tillhör generation 3 och har nollställts i samband med den svekonorvegiska orogenesen eller att kalifältspaten är svekonorvegisk.

Contents

1	Introduction	7
2	Objective and scope	9
3	Equipment	11
3.1	Description of equipment/interpretation tools	11
4	Execution	13
4.1	Selection of samples	13
4.2	Preparations	13
4.3	Execution of field work	13
4.4	Analyses and interpretations	13
4.5	Nonconformities	14
5	Results	15
5.1	Sample KA1755A: 211.70–211.75 m (muscovite)	15
5.2	Sample KSH01A: 256.90–257.10 m (adularia)	15
5.3	Sample KSH03B: 14.97–15.32(I) m (adularia)	17
5.4	Sample KSH03A: 181.93–181.98 m (adularia)	18
5.5	Sample KSH03A: 186.52–186.62 m (illite)	20
5.6	Sample KSH03A: 863.66–863.84 m (adularia)	21
5.7	Sample KLX02: 676.82–677.00 m (apophyllite)	23
5.8	Sample KLX03: 722.72–722.96 m (muscovite)	25
5.9	Sample KLX03: 970.04–970.07 m (apophyllite)	27
5.10	Sample KLX06: 535.10–535.26 m (muscovite)	29
5.11	Sample KLX06: 565.22–565.38 m (muscovite)	30
5.12	Sample KLX06: 595.08–595.18 m (muscovite)	31
5.13	Sample KLX08: 933.15–933.30 m (hornblende)	32
6	Summary and discussions	35
7	Acknowledgements	37
8	References	39
Appendix 1	$^{40}\text{Ar}/^{39}\text{Ar}$ -data	41

1 Introduction

This document reports $^{40}\text{Ar}/^{39}\text{Ar}$ dating results from fracture minerals. Samples are from the Laxemar and Simpevarp subareas and Äspö. The work was carried out in accordance with activity plan AP PS 400-06-158. In Table 1-1 controlling documents for performing this activity are listed. Both activity plan and method descriptions are SKB's internal controlling documents.

A relative, geochronological sequence of fracture minerals based on e.g. cross-cutting relations in about 200 drill core samples from more than 10 different cored boreholes has been established. This sequence comprises seven generations and is common for the Simpevarp and Laxemar sub-areas and Äspö. Detailed descriptions of the fracture mineralogy and the sequences and paragenesis have earlier been reported; Simpevarp subarea /Drake and Tullborg 2004, 2006a/, Laxemar subarea /Drake and Tullborg 2005, 2007/ and Äspö /Drake and Tullborg 2005/. Stable isotope analyses on calcite, pyrite, barite and gypsum and geochemical analyses have further contributed to the subdivision into different fracture mineral generations. The fracture mineral generations grade from relatively high temperature (greenschist facies) to low temperature (zeolite facies down to ambient temperatures). They are summarized in Table 1-2 (modified from/Drake and Tullborg 2007/).

$^{40}\text{Ar}/^{39}\text{Ar}$ dating has been performed on samples from generation 1, 3, 5 and 6 and on muscovite in the red-stained wall rock adjacent to a fracture filled with minerals of generation 3 and 4. Three samples of coarse-grained muscovite in greisen-like fractures (thought to be coeval with generation 3) from KLX06 have also been dated. Each sample is found in Table 1-3.

Table 1-1. Controlling documents for the performance of the activity.

Activity plan	Number	Version
Geokronologisk undersökning av sprickmineral	AP PS 400-06-158	1.0
Method descriptions	Number	Version
Sprickmineralogi	SKB MD 144.000	1.0
Åldersdateringar av mineral och bergarter	SKB MD 132.002	

Table 1-2. Schematic fracture filling-sequence from Simpevarp/Laxemar/Äspö. The most abundant minerals in each generation are in bold letters. Minerals in brackets are only found occasionally.

1. **Quartz- and epidote-rich mylonite**, including muscovite, titanite, Fe-Mg-chlorite, albite, (apatite, calcite and K-feldspar)
2. **Cataclasite**
 - a. Early green coloured; **epidote-rich**, with **quartz, Fe-Mg-chlorite**, (titanite, K-feldspar, and albite)
 - b. Late red-brown colour; **K-feldspar, chlorite, quartz, hematite**, albite, (and illite)
3. Euhedral **quartz, epidote, Fe-Mg chlorite, calcite**, pyrite, fluorite, muscovite, (K-feldspar and hornblende)
4. **Prehnite**, (fluorite)
5.
 - a. **Calcite**, (fluorite and hematite)
 - b. **Dark red/brown filling - Adularia, Mg-chlorite, hematite**; sometimes cataclastic.
 - c. **Calcite, adularia, laumontite, Mg-chlorite, quartz, illite, hematite**, (ML-clay – chlorite/illite, albite and apatite)
6. **Calcite, adularia, Fe-chlorite, hematite, fluorite, quartz, pyrite, barite, gypsum, corrensite** (and other types of mixed-layer clay), harmotome, REE-carbonate, galena, apophyllite, illite, chalcopyrite, sphalerite, U-silicate, Cu(Zn,Ni,Sn,Fe)-rich minerals, apatite, laumontite (Ti-oxide, Mg-chlorite and albite)
7. **Calcite**, pyrite, Fe-oxyhydroxide (near surface)

The original results are stored in the primary data base (SICADA) and are traceable by the activity plan number 400-06-158.

Table 1-3.

Sample	Dated mineral	Generation	Report
KA1755A: 211.70–211.75 m	Muscovite	1	/Drake and Tullborg 2005/
KSH01A: 256.90–257.10 m	Adularia	6	/Drake and Tullborg 2004/
KSH03B: 14.97–15.32(l) m	Adularia	6	/Drake and Tullborg 2006a/
KSH03A: 181.93–181.98 m	Adularia	6	/Drake and Tullborg 2006a/
KSH03A: 186.52–186.62 m	Illite	5 or 6	/Drake and Tullborg 2006a/
KSH03A: 863.66–863.84 m	Adularia	3 or later	/Drake and Tullborg 2006a/
KLX02: 676.82–677.00 m	Apophyllite	6	/Drake and Tullborg 2005/
KLX03: 722.72–722.96 m	Muscovite	3 or 4 (wall rock)	/Drake and Tullborg 2007/
KLX03: 970.04–970.07 m	Apophyllite	6	/Drake and Tullborg 2007/
KLX06: 535.10–535.26 m	Muscovite	Greisen fractures	/Drake and Tullborg 2007/
KLX06: 565.22–565.38 m	Muscovite	Greisen fractures	/Drake and Tullborg 2007/
KLX06: 595.08–595.18 m	Muscovite	Greisen fractures	/Drake and Tullborg 2007/
KLX08: 933.15–933.30 m	Hornblende	3	/Drake and Tullborg 2007/

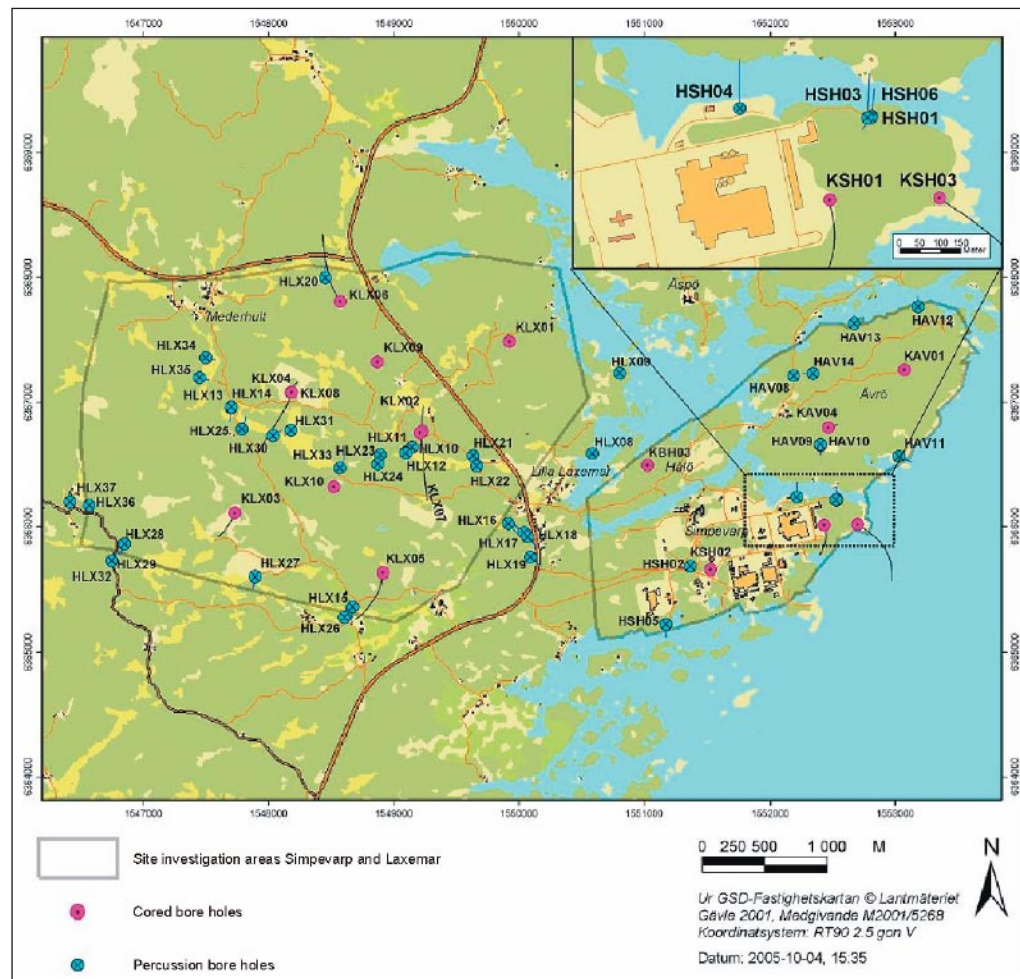


Figure 1-1. General overview of the Simpevarp site investigation area, with cored and percussion drill holes shown. Drill hole KA1755A is not shown (it is from the tunnel at Åspö).

2 Objective and scope

The objective is to provide absolute geochronological constraints for the relative sequence of fracture generations that has been established in the Simpevarp area /Drake and Tullborg 2004, 2005, 2006a, 2007/ and thereby contribute to the interpretation of the geological evolution of the area.

This report presents the data obtained from $^{40}\text{Ar}/^{39}\text{Ar}$ dating but no detailed interpretation of the geological evolution is reported.

3 Equipment

3.1 Description of equipment/interpretation tools

- Rock saw
- Swing mill
- Tweezers
- Digital camera
- Petrographic Microscope (Leica DMRXP)
- Binocular microscope (Leica MZ12)
- Digital microscope camera (Leica DFC 280)
- Scanning electron microscope (HITACHI S-3400N)
- EDS-detector (INCA DryCool)

All the equipment described above is property of the Earth Sciences Centre, Göteborg University, Sweden. For the geochronological analyses the following equipment was used:

- Micromass 5400 mass spectrometer (Lund University, Sweden)
- New Wave Research 50W CO₂ laser facility (Lund University, Sweden)

4 Execution

4.1 Selection of samples

The selection of samples for dating is a delicate issue. Pure minerals that can be found in paragenesis are difficult to sample. Instead several minerals, sometimes from several generations found in the same fracture are the common case. Before the selection of samples for geochronological analyses, thin sections and fracture surface samples were examined using binocular microscope, petrographic microscope and scanning electron microscope (SEM-EDS) in order to identify suitable fracture minerals. The samples finally selected belonged to drill cores from KA17755A, KSH01A, KSH03A+B, KLX02, KLX03, KLX06 and KLX08.

4.2 Preparations

From sealed fractures, the fracture filling was separated from the wall rock using a rock saw and then crushed manually with a hammer or the fracture filling was removed from the sample with a knife. The fragments were put in a swing mill for a few seconds to obtain small grains made up of individual mineral phases. The mineral was then handpicked with tweezers under a binocular microscope.

Apophyllite crystals were handpicked from the fracture surface under a binocular microscope.

4.3 Execution of field work

Samples have been selected from drill cores from the cored boreholes KLX02, KA17755A, KSH01A, KSH03A+B, KLX03, KLX06 and KLX08 during the sampling for the detailed fracture mineralogy studies (activities AP PS 400-03-045, AP PS 400-05-053 and AP PS 400-05-074).

4.4 Analyses and interpretations

The samples selected for $^{40}\text{Ar}/^{39}\text{Ar}$ geochronology were irradiated together with the 28.34 TCR sanidine standard (28.34 Ma recalculated following /Renne et al. 1998/, for 35 hours at the NRG-Petten HFR RODEO facility in the Netherlands. J-Values were calculated with a precision of 0.25%.

The $^{40}\text{Ar}/^{39}\text{Ar}$ geochronology laboratory at Lund University contains a Micromass 5400 mass spectrometer with a Faraday and an electron multiplier. A metal extraction line, which contains two SAES C50-ST101 Zr-Al getters and a cold finger cooled to ca -155°C by a Polycold P100 cryogenic refrigeration unit, is also present. One or two grains of adularia were loaded into a copper planchette that consists of several 3 mm holes. Samples were step-heated using a defocused 50W CO₂ laser. Sample clean-up time that made use of the two hot Zr-Al SAES getters and a cold finger with a Polycold refrigeration unit was five minutes. The laser was rastered over the samples to provide even-heating of all grains. The entire analytical process is automated and runs on a Macintosh-steered OS 10.2 with software modified specifically for the laboratory at Lund University. The software was originally developed at the Berkeley geochronology Centre (Al Deino). 18 Time zero regressions were fitted to data collected from 10 scans over the mass range of 40 to 36. Peak heights and backgrounds were corrected for mass discrimination, isotopic decay and interfering nucleogenic Ca-, K-, and Cl-derived

isotopes. Isotopic production values for the cadmium-lined position in the Petten reactor are $^{36}\text{Ar}/^{37}\text{Ar}(\text{Ca}) = 0.000270$, $^{39}\text{Ar}/^{37}\text{Ar}(\text{Ca}) = 0.000699$, and $^{40}\text{Ar}/^{39}\text{Ar}(\text{K}) = 0.00183$. ^{40}Ar blanks were calculated before every new sample and after every three sample steps. ^{40}Ar blanks were between $6.0^{-3} \times 10^{-16}$. Blank values for masses 39–36 were all less than 7×10^{-18} . Blank values were subtracted for all incremental steps from the sample signal. The laboratory was able to produce very good incremental gas splits, using a combination of increasing time at the same laser output, followed by increasing laser output. Age plateaus were determined using the criteria of /Dalrymple and Lanphere 1971/, which specify the presence of at least three contiguous incremental heating steps with statistically indistinguishable ages and constituting greater than 50% of the total ^{39}Ar released during the experiment.

4.5 Nonconformities

Three of the samples did not yield plateau ages and one sample gave a very unrealistic age (too young).

5 Results

5.1 Sample KA1755A: 211.70–211.75 m (muscovite)

The sample consists of mylonite (generation 1) from the Äspö Shear Zone (ZSMNE005A). Minerals present are muscovite, quartz, epidote, K-feldspar, albite and some titanite. The mylonite is cut by a fracture filled with calcite, fluorite and hematite.

The plateau age of muscovite defined on the $^{40}\text{Ar}/^{39}\text{Ar}$ step-heating spectrum is $1\,406 \pm 3$ Ma (Figure 5-2). This age is however younger than expected. The mylonites in the area are commonly thought to be older than the granite intrusions at Götemar ($1,452 +11/-9$ Ma, /Åhäll 2001/) and Uthammar ($1,441 +5/-3$ Ma, /Åhäll 2001/) nearby /Nisca 1987, Talbot and Riad 1988/. The age obtained for the muscovite from drill core KA1755A may thus represent re-activation of the mylonite and formation of muscovite at the time of the intrusion of these granites. However, it is more likely that the muscovite existed before the intrusions of the granites and that the obtained age represents heating of the muscovite above its Ar-blocking temperature ($\sim 350^\circ\text{C}$) in connection with the intrusions of the Götemar and Uthammar granites.

5.2 Sample KSH01A: 256.90–257.10 m (adularia)

The adularia is found in sealed fractures (generation 6) together with calcite, Mg-rich chlorite, Fe-rich chlorite, pyrite etc. These fractures cut through brown-coloured cataclasite, which is composed of adularia, Mg-rich chlorite and hematite.

The plateau age defined on the $^{40}\text{Ar}/^{39}\text{Ar}$ step-heating spectrum is 425.8 ± 1.7 Ma (Figure 5-5). The age is interpreted as the crystallization age of the adularia.



Figure 5-1. KA1755A: 211.70–211.75 m. Mylonite (generation 1), cut by a fracture filled with calcite (white), fluorite and hematite.

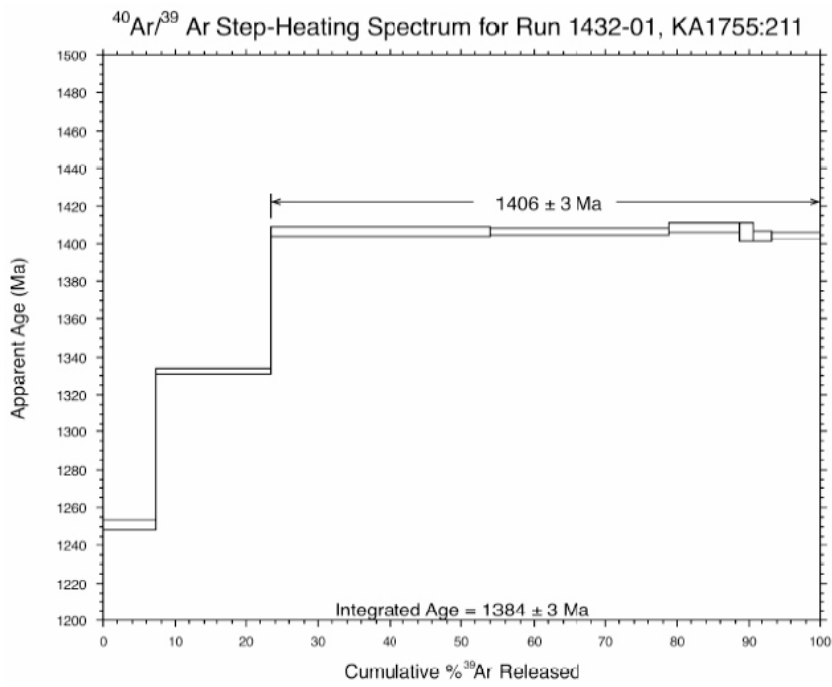


Figure 5-2. $^{40}\text{Ar}/^{39}\text{Ar}$ muscovite step-heating spectrum for sample KA1755A: 211.70–211.75 m.



Figure 5-3. Sample KSH01A: 256.90–257.10 m. Sealed fractures (generation 6), filled with calcite, adularia, Mg-chlorite, Fe-chlorite and pyrite etc. are cutting through brown-coloured cataclasite.

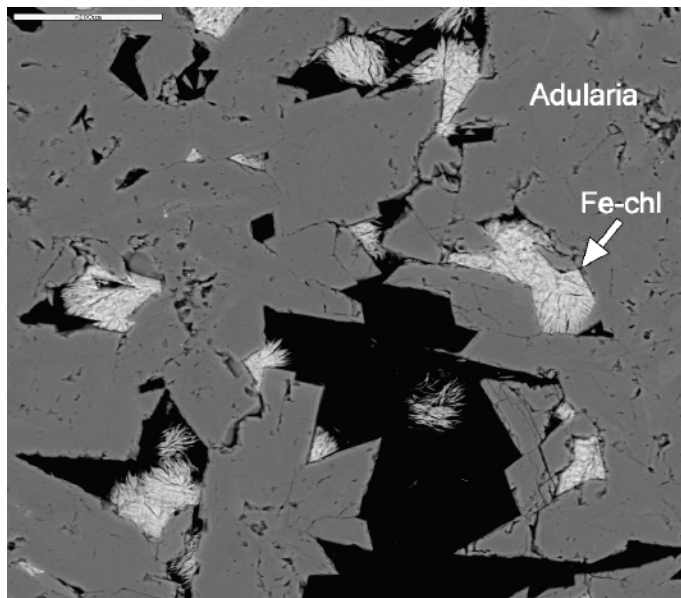


Figure 5-4. Sample KSH01A: 256.90–257.10 m. Back-scattered SEM-image of adularia and Fe-rich chlorite (Fe-chl).

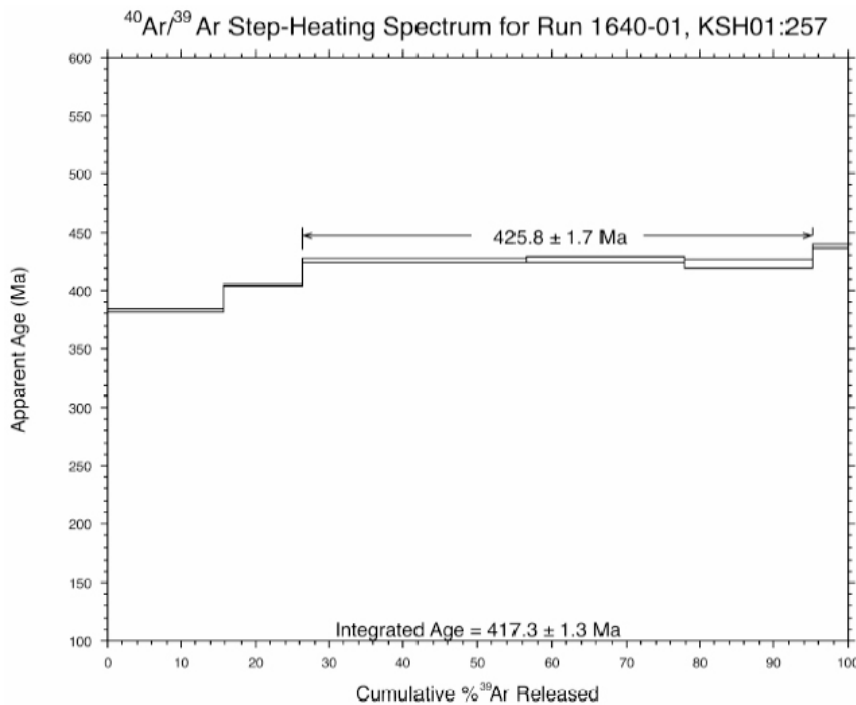


Figure 5-5. $^{40}\text{Ar}/^{39}\text{Ar}$ adularia step-heating spectrum for sample KSH01A: 256.90–257.10 m.

5.3 Sample KSH03B: 14.97–15.32(l) m (adularia)

Sealed fracture mainly filled with adularia and subordinate calcite and hematite.

The plateau ages defined on the $^{40}\text{Ar}/^{39}\text{Ar}$ step-heating spectrums are 443.3 ± 1.2 Ma (Split 1, Figure 5-8) and 448.0 ± 1.2 Ma (Split 2, Figure 5-9). The age span of 443–448 Ma is interpreted as the crystallization age of the adularia. This age span is consistent with the “warm brine” origin of co-precipitated calcite, revealed by stable isotope analysis (C and O). These fluids were interpreted to have formed during the Palaeozoic /Drake and Tullborg 2006a/.

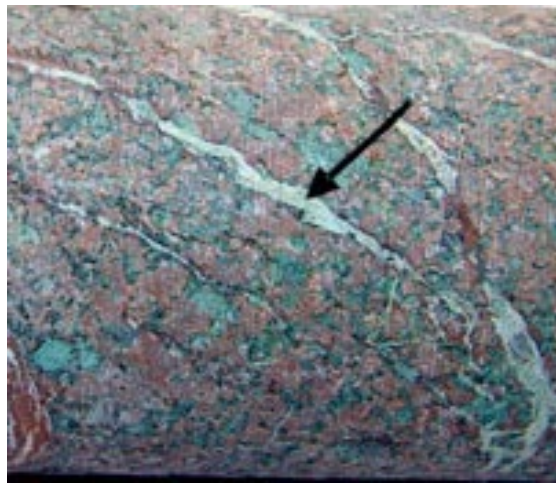


Figure 5-6. Sealed fracture filled with adularia, calcite and hematite.

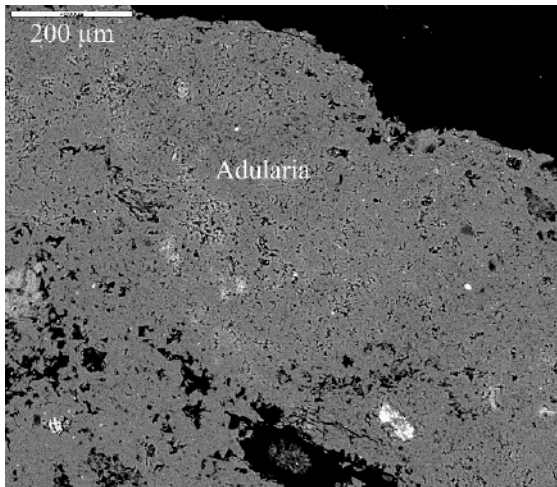


Figure 5-7. Back-scattered SEM-image of adularia in the sealed fracture.

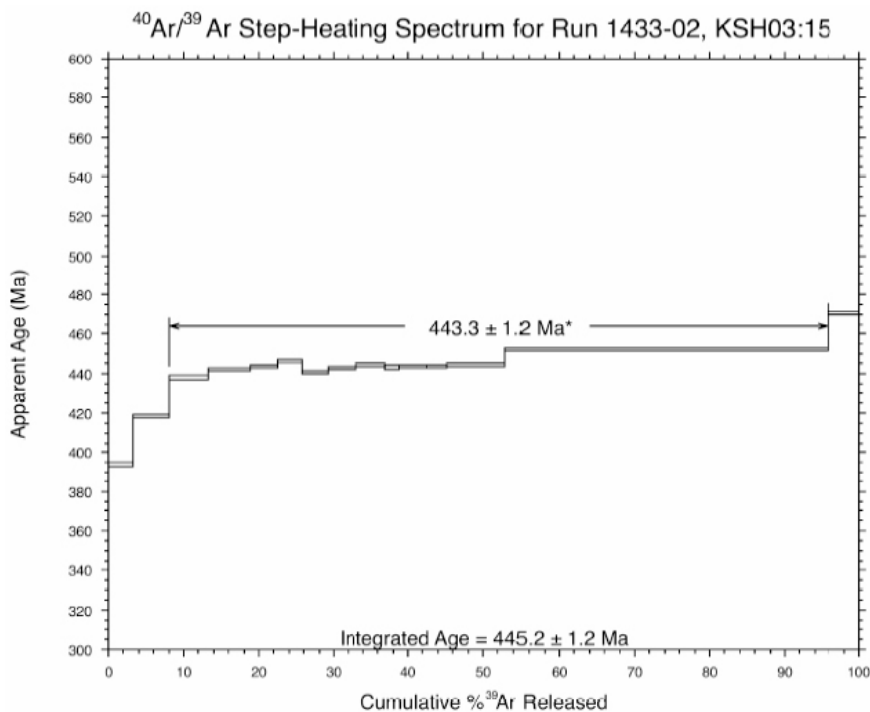


Figure 5-8. $^{40}\text{Ar}/^{39}\text{Ar}$ adularia step-heating spectrum for sample KSH03B: 14.97–15.32(I) m. Split 1.

5.4 Sample KSH03A: 181.93–181.98 m (adularia)

The sample consists of sealed fractures of several generations. The first generation is cataclasite (generation 2) which is cut by calcite-filled fractures (generation 3). The latest formed fractures are filled with adularia (generation 6) and laumontite. It is difficult to discern in thin-section if adularia and laumontite are coeval. There exist fragments of calcite within the adularia filling. This calcite has stable isotope ratios which are similar to generation 3–4 calcite.

The plateau age defined on the $^{40}\text{Ar}/^{39}\text{Ar}$ step-heating spectrum is 400.9 ± 1.1 Ma (Figure 5-12). The plateau age is interpreted as the crystallization age of the adularia and is a maximum age of the laumontite in the same fracture since the laumontite is found in the centre of the adularia-coated fracture.

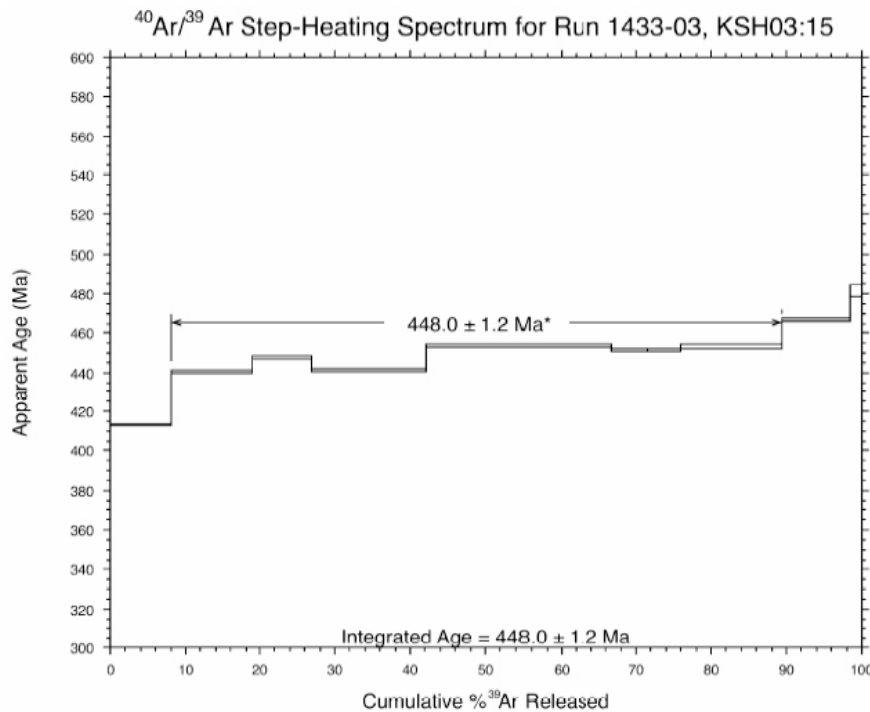


Figure 5-9. $^{40}\text{Ar}/^{39}\text{Ar}$ adularia step-heating spectrum for sample KSH03B: 14.97–15.32(I) m. Split 2.

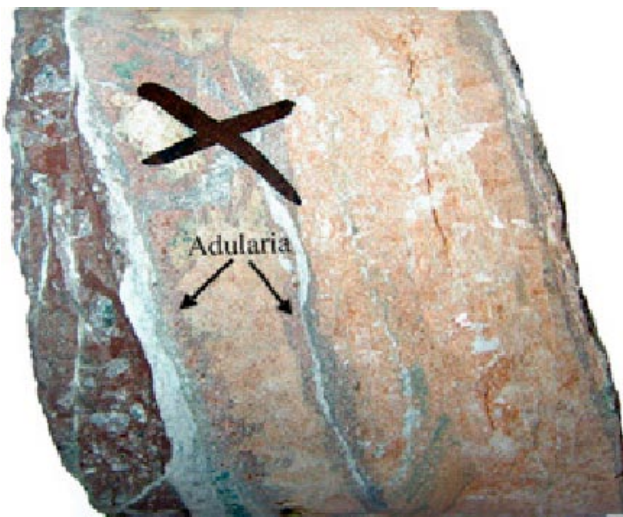


Figure 5-10. Cataclasite (generation 2, red-brown coloured, left) is cut by calcite-filled fractures (generation 3, white colour). The latest formed fractures are filled with adularia (generation 6) and laumontite, (orange colour).

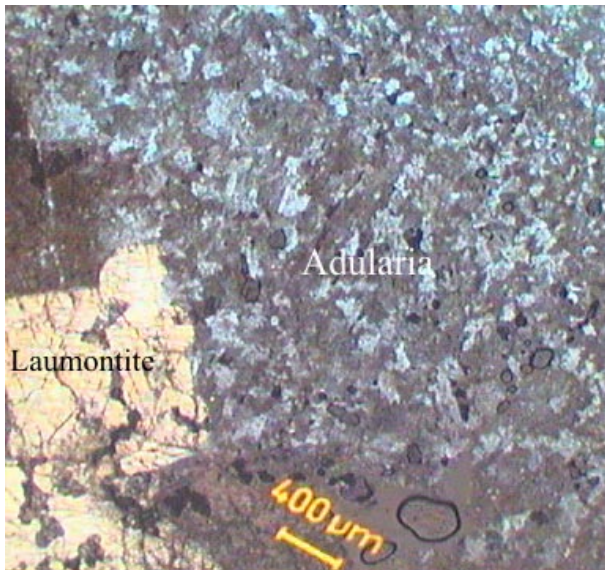


Figure 5-11. Photomicrograph of adularia and laumontite (at the right arrow in Figure 5-10 above).

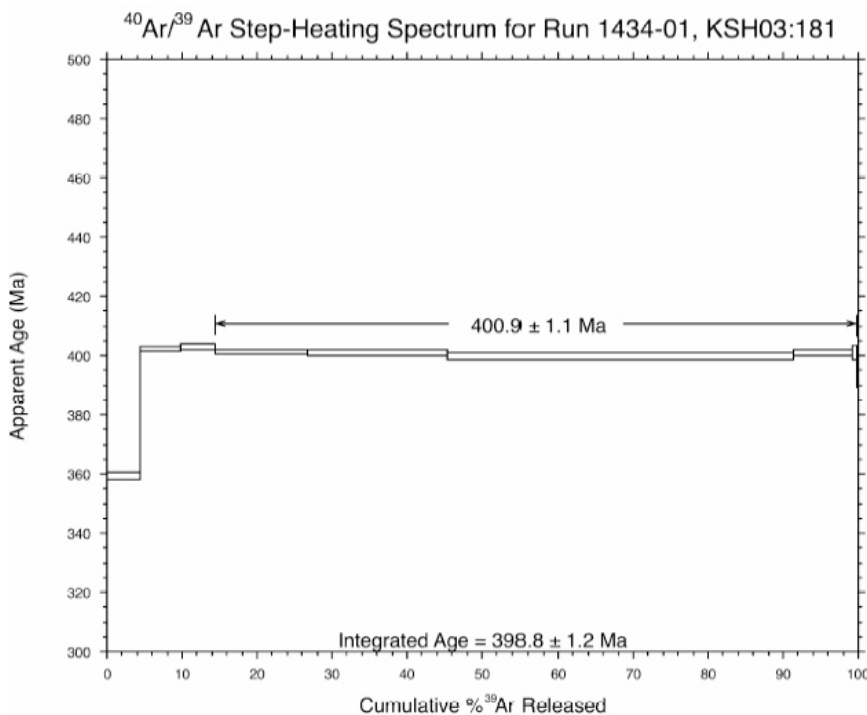


Figure 5-12. $^{40}\text{Ar}/^{39}\text{Ar}$ adularia step-heating spectrum for sample KSH03A: 181.93–181.98 m.

5.5 Sample KSH03A: 186.52–186.62 m (illite)

A dark green illite-rich fracture filling is cut by sealed fractures filled with calcite (“warm brine” origin) and small amounts of adularia.

The illite sample did not yield a plateau age. However, the integrated age (488.5 ± 1.1 Ma, Figure 5-14) defined on the $^{40}\text{Ar}/^{39}\text{Ar}$ step-heating spectrum might give a speculative indication of the age of the mineral /cf. p. 36–37 in McDougall and Harrison 1999/. The integrated age for the illite would be reasonable since it is cut by Palaeozoic calcite of generation 6, a generation that is dated to 400–448 Ma (this report and /Sundblad et al. 2004/).



Figure 5-13. Dark green illite-rich fracture filling cut by sealed fractures filled with calcite and small amounts of adularia.

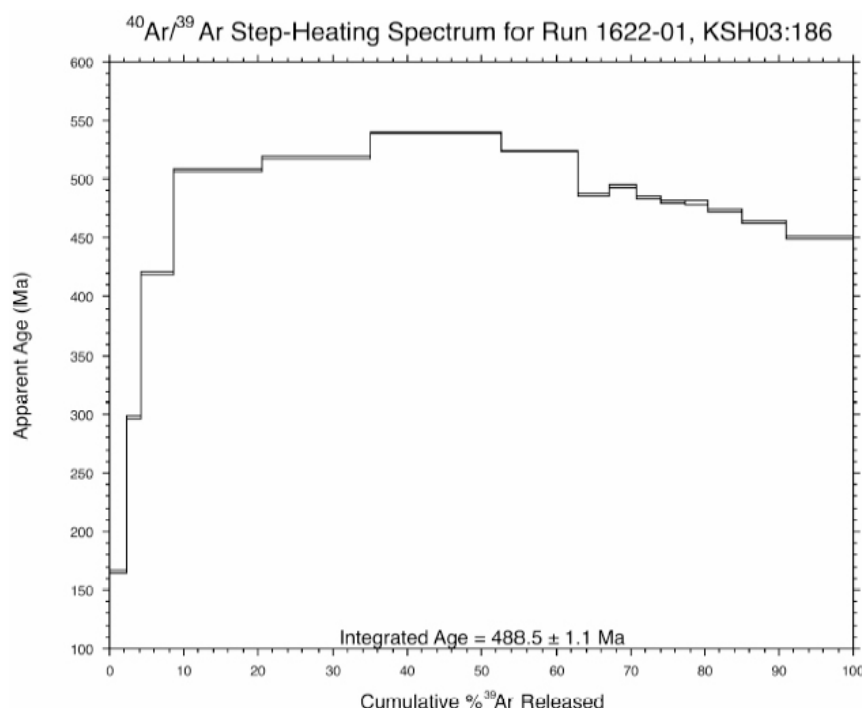


Figure 5-14. $^{40}\text{Ar}/^{39}\text{Ar}$ illite step-heating spectrum for sample KSH03A: 186.52–186.62 m.

5.6 Sample KSH03A: 863.66–863.84 m (adularia)

The sample consists of a more than 20 centimetre wide light green mylonite/cataclasite (generation 1 or 2) including wall rock fragments. Two sets of thin (< 1 millimetre) fractures cut the mylonite/cataclasite. The mylonite/cataclasite matrix consists of about 80–90% of fine-grained epidote and the rest is K-feldspar and quartz.

The fractures cutting the mylonite/cataclasite are filled with K-feldspar (probably adularia), quartz and occasionally chlorite. When chlorite, K-feldspar and quartz appear in the same fracture, the chlorite is present in the centre of the fracture whereas the K-feldspar and quartz coat the fracture walls. The chlorite is of Fe-Mg-type (as common in generation 3 and earlier).



Figure 5-15. K-feldspar (red), quartz and chlorite (black) in fractures that cut through mylonite/cataclasite. Photograph from a sawed piece of the sample.

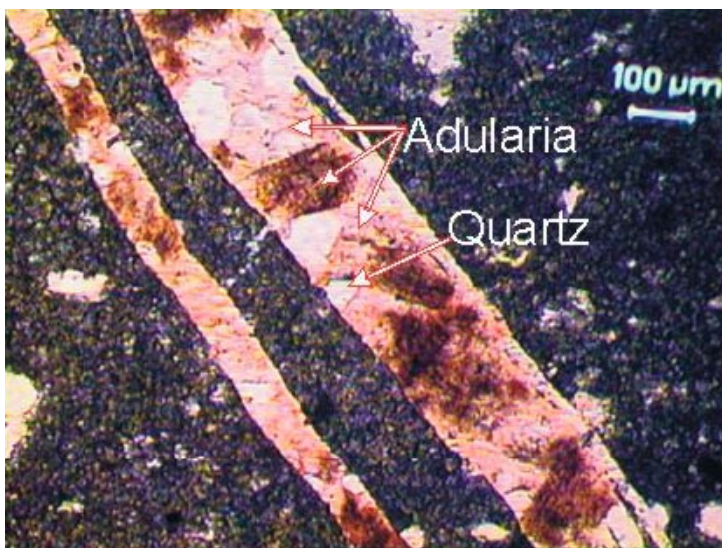


Figure 5-16. Microphotograph of adularia and quartz in fractures that cut through mylonite/cataclasite.

The plateau age defined on the $^{40}\text{Ar}/^{39}\text{Ar}$ step-heating spectrum is 989 ± 2 Ma (Figure 5-17). The left hand side of the spectrum most likely indicates slow cooling of multi diffusion domain K-feldspars. The plateau age can be interpreted as either crystallization of the K-feldspar or complete resetting of an older K-feldspar during a Sveconorwegian event. This means that it can either be a generation 3 K-feldspar that has been reset or that the K-feldspar was formed in connection with the Sveconorwegian orogeny (this K-feldspar is classified as a generation 3 mineral, based on the chemistry of the related chlorite).

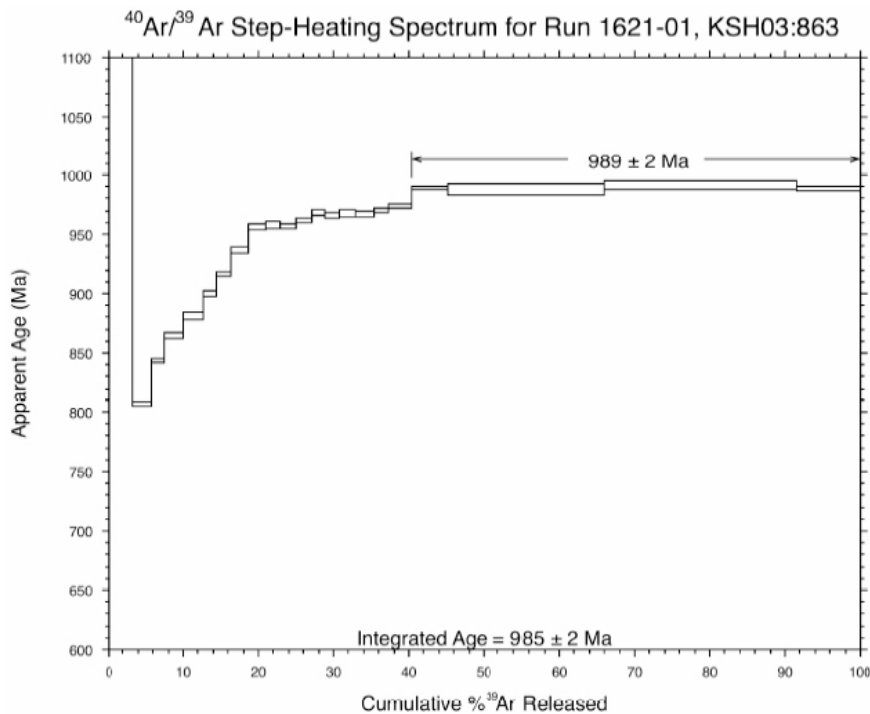


Figure 5-17. $^{40}\text{Ar}/^{39}\text{Ar}$ adularia step-heating spectrum for sample KSH03A: 863.66–863.84 m.

5.7 Sample KLX02: 676.82–677.00 m (apophyllite)

Open fracture coated by euhedral apophyllite and barite of generation 6.

The sample yielded plateau ages (two splits, Figures 5-19 and 5-20) but these ages are much lower than expected and this is probably due to the observed decomposition of the apophyllite during the analyses. These ages are thus considered to be insignificant.

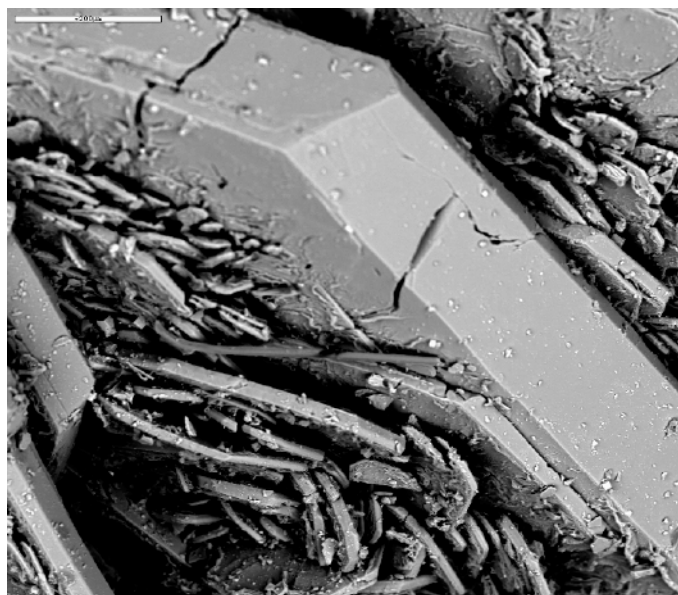


Figure 5-18. Sample KLX02: 676.82–677.00 m.

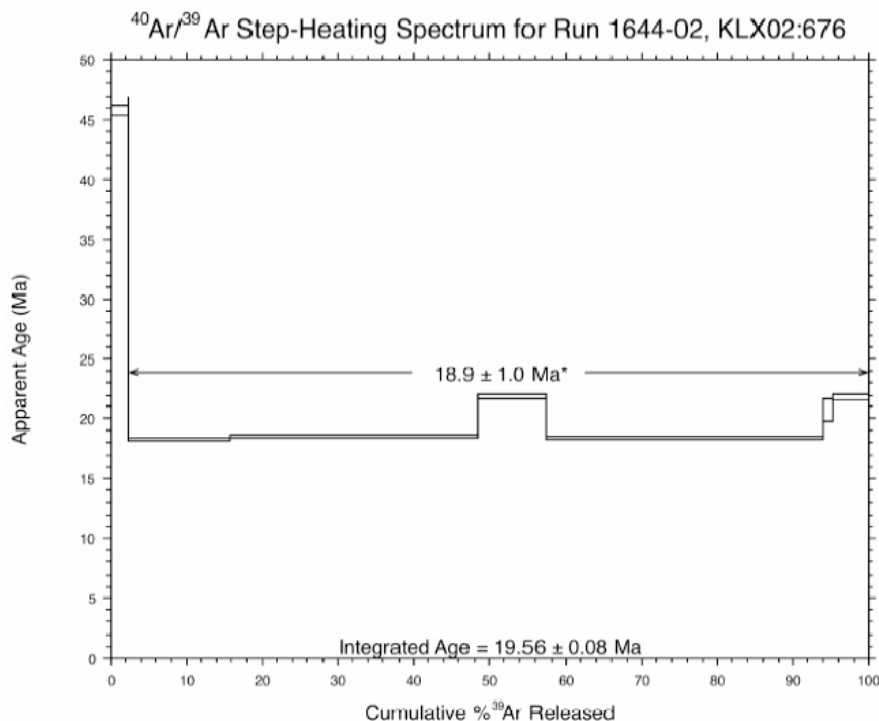


Figure 5-19. ⁴⁰Ar/³⁹Ar apophyllite step-heating spectrum for sample KLX02: 676.82–677.00 m. Split 1.

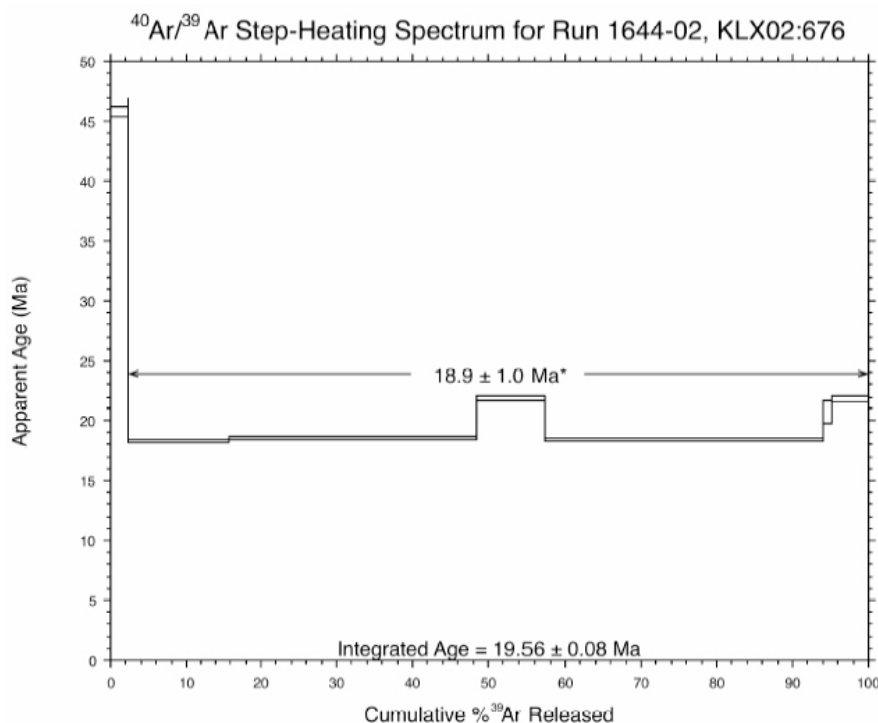


Figure 5-20. ⁴⁰Ar/³⁹Ar apophyllite step-heating spectrum for sample KLX02: 676.82–677.00 m. Split 2.

5.8 Sample KLX03: 722.72–722.96 m (muscovite)

The fracture filling is 10–15 mm thick and consists of dominantly Fe-Mg chlorite, quartz and calcite (generation 3). The fracture has later been re-activated and a 5 millimetre wide fracture filled with prehnite (generation 4) cuts through the chlorite-quartz-calcite filling.

The wall rock is bleached close to the filled fracture, and more reddish 1–2 centimetres away from the fracture. The colour in these sections depends on the features of the plagioclase alteration; 1) in the red coloured part the pseudomorphs after plagioclase consist of albite, K-feldspar, muscovite (sericite) and prehnite. The red colour originates from minute hematite crystals in micro-pores in the secondary minerals in the pseudomorphs after plagioclase. 2) In the bleached parts, the plagioclase pseudomorphs consist of albite, prehnite and euhedral muscovite.

Most biotite is replaced by chlorite. The dated sample consists of muscovite from pseudomorphs after plagioclase in the bleached part of the rock. The bleaching and red-staining of the wall rock are thought to be related to the same event because many fractures filled with minerals of one generation only (often prehnite) show bleached rock close to the fracture and red-stained rock further away from the fracture. The different colours (bleached or red-stained) may depend on distance from the fracture, temperature, or fluid chemistry etc.

The plateau age defined on the $^{40}\text{Ar}/^{39}\text{Ar}$ step-heating spectrum is $1,417 \pm 3$ Ma (Figure 5-23). It is interpreted as the crystallization age of the muscovite. This is also thought to be the age of the fracture minerals of generations 3 and 4 (epidote, chlorite, quartz, calcite, prehnite). The assumption that generations 3 and 4 are of essentially the same age is based on that both generations fill fractures bordered by red-stained wall rock and, furthermore, the two generations show identical stable and Sr isotope results for calcites /Drake and Tullborg 2006a, 2007/. The obtained age of these fillings indicate that they are related to the intrusions (or post-magmatic fluid circulation) of the Götemar and Uthammar granites as shown by e.g. ages of muscovite in greisen-like fractures closer to the Götemar granite (see Section 5.9, 5.10, 5.11). The age of the muscovite also indicate that the major part of the extensive red-staining of the rocks in the area, studied by /Eliasson 1993, Drake and Tullborg 2006cd/, is related to these intrusions and/or related post-magmatic circulation.



Figure 5-21. Photograph of the drill core showing a fracture sealed with calcite, quartz and chlorite and subsequently prehnite. The red-stained wall rock is bleached close to the fracture, due to a high amount of muscovite in the altered plagioclase.

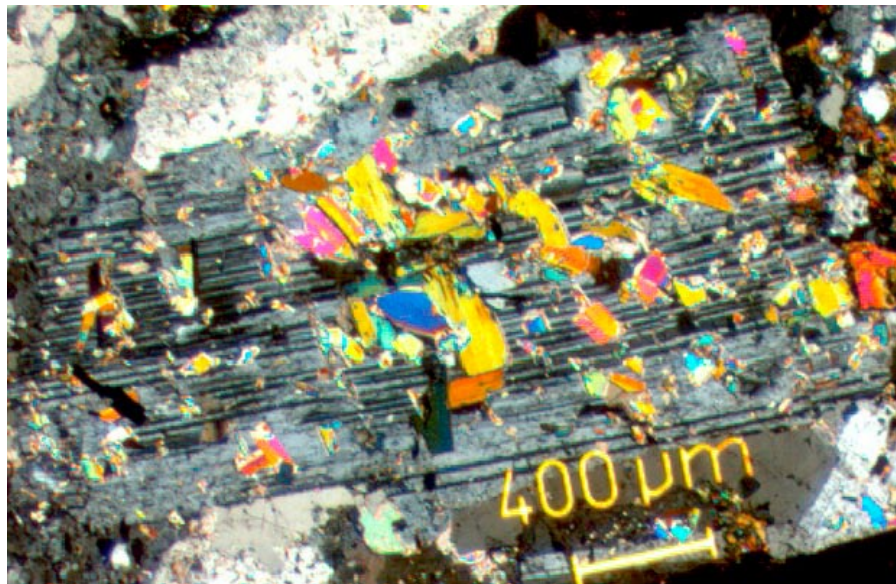


Figure 5-22. Photomicrograph of an altered plagioclase crystal with muscovite crystals in it.

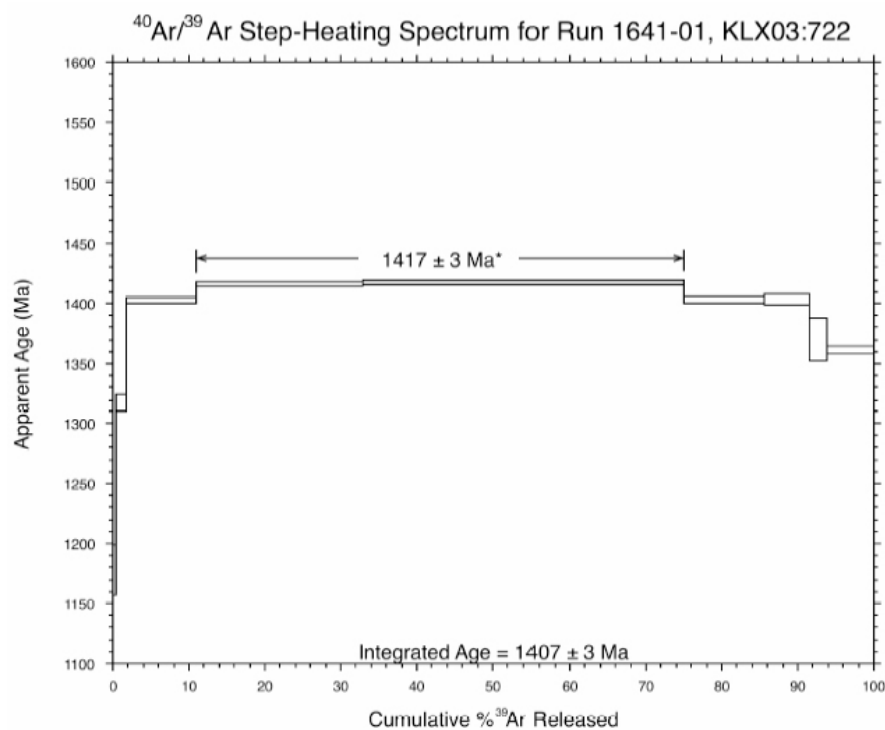


Figure 5-23. ⁴⁰Ar/³⁹Ar muscovite step-heating spectrum for sample KLX03: 722.72–722.96 m.

5.9 Sample KLX03: 970.04–970.07 m (apophyllite)

The sample consists of an open fracture coated by euhedral apophyllite of generation 6. Small amounts of calcite and barite are also present. The sample did not yield a plateau age.



Figure 5-24. Photograph of the fracture surface covered with apophyllite.



Figure 5-25. Back-scattered SEM-image of apophyllite on the fracture surface. Scale marker is ~ 200 μm .

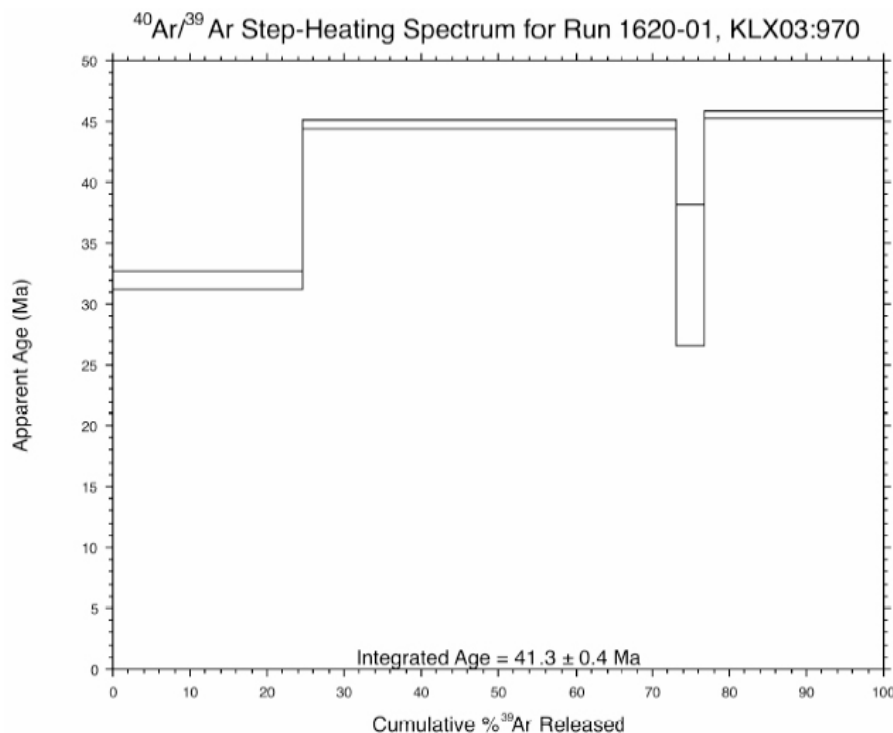


Figure 5-26. ⁴⁰Ar/³⁹Ar apophyllite step-heating spectrum for sample KLX03: 970.04–970.07 m. Split 1.

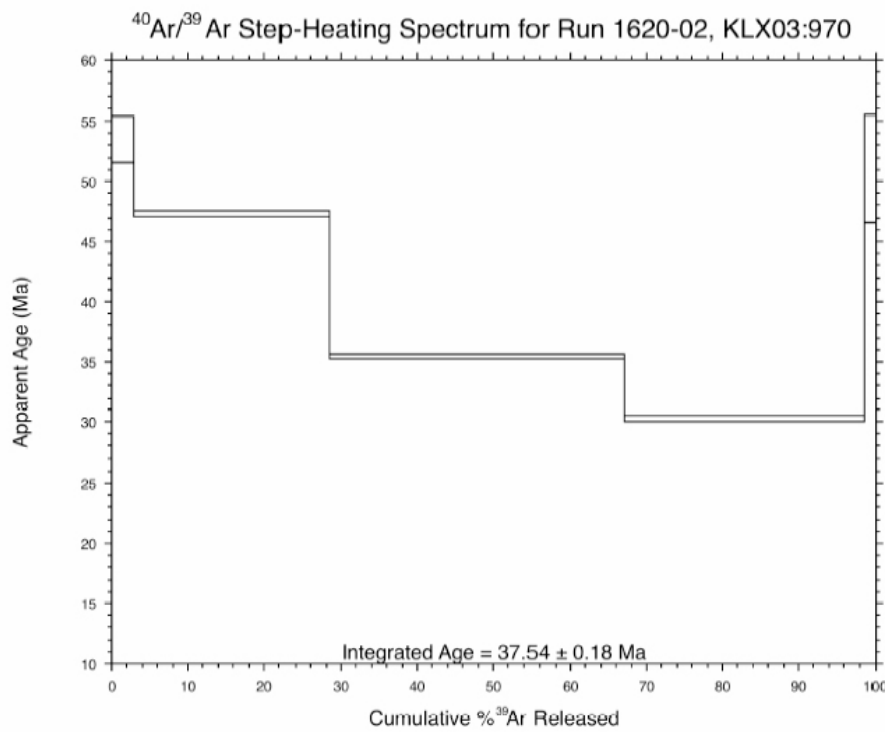


Figure 5-27. ⁴⁰Ar/³⁹Ar apophyllite step-heating spectrum for sample KLX03: 970.04–970.07 m. Split 2.

5.10 Sample KLX06: 535.10–535.26 m (muscovite)

Sealed fracture (2–3 cm wide) coated by coarse-grained muscovite and filled with coarse-grained pyrite and small amounts of calcite. Diffuse contact to the wall rock, which is strongly sericitized.

The plateau age defined on the $^{40}\text{Ar}/^{39}\text{Ar}$ step-heating spectrum is $1,424 \pm 2$ Ma (Figure 5-29). It is interpreted as the crystallization age of the muscovite. This age shows that these fillings are related to the intrusion (and/or post-magmatic circulation) of the Götemar granite. The somewhat lower age (minimum ~ 20 Ma) for the muscovite than for the intrusion of the Götemar granite ($1,452 +11/-9$ Ma, /Åhäll 2001/) might be due to formation of muscovite related to post-magmatic circulation and that the closure temperature for Ar is quite low in muscovite ($\sim 350^\circ\text{C}$).



Figure 5-28. Photograph of the drill core showing a fracture sealed with muscovite, pyrite, quartz and calcite (not visible in the photograph).

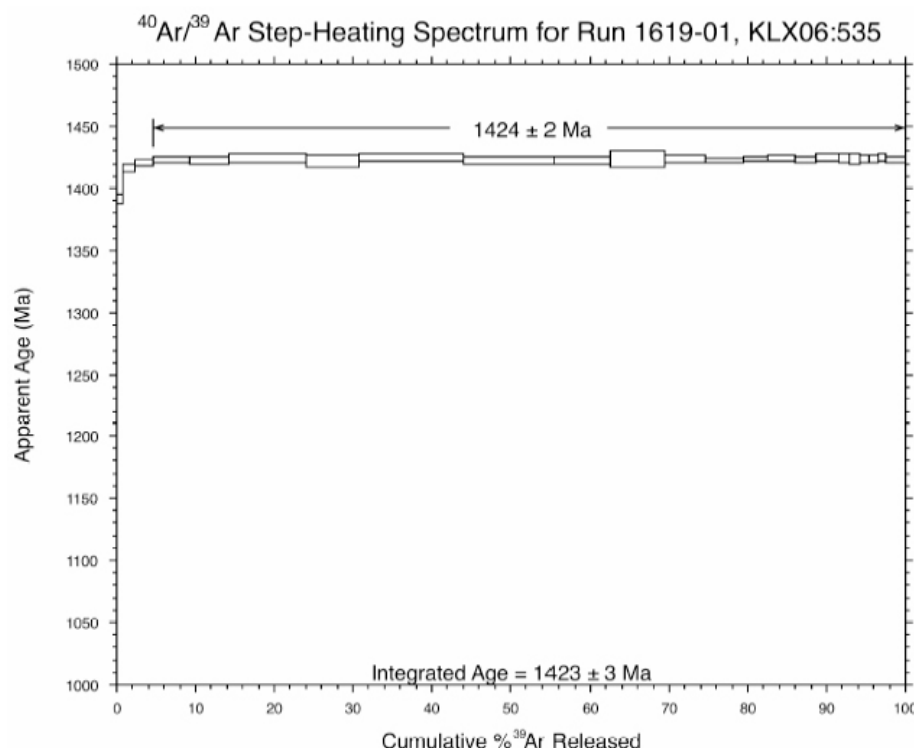


Figure 5-29. $^{40}\text{Ar}/^{39}\text{Ar}$ muscovite step-heating spectrum for sample KLX06: 535.10–535.26 m.

5.11 Sample KLX06: 565.22–565.38 m (muscovite)

Sealed fracture (about 10 cm wide), filled with coarse-grained quartz, muscovite and fluorite. Diffuse contact to the wall rock, which is strongly sericitized.

The plateau age defined on the $^{40}\text{Ar}/^{39}\text{Ar}$ step-heating spectrum is $1,423 \pm 3$ Ma (Figure 5-31). It is interpreted as the crystallization age of the muscovite. This age shows that these fillings are related to the intrusion (and/or post-magmatic circulation) of the Götemar granite. The somewhat lower age (minimum ~ 20 Ma) for the muscovite than for the intrusion of the Götemar granite ($1,452 +11/-9$ Ma, /Åhäll 2001/) might be due to formation of muscovite related to post-magmatic circulation and that the closure temperature for Ar is quite low in muscovite ($\sim 350^\circ\text{C}$).



Figure 5-30. Photograph of the drill core showing a fracture sealed with muscovite, quartz and fluorite.

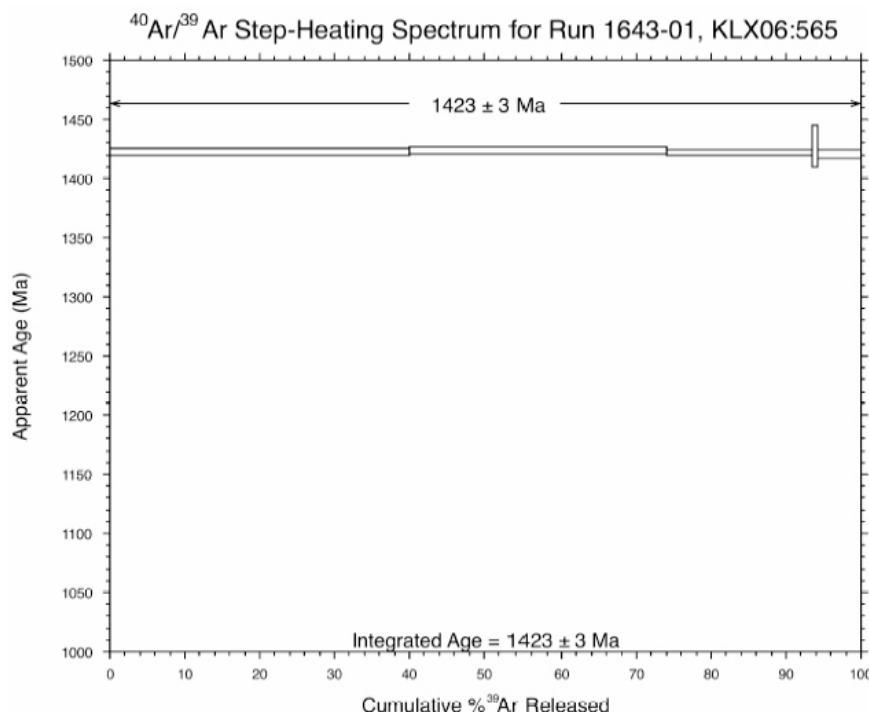


Figure 5-31. $^{40}\text{Ar}/^{39}\text{Ar}$ muscovite step-heating spectrum for sample KLX06: 565.22–565.38 m.

5.12 Sample KLX06: 595.08–595.18 m (muscovite)

Sealed fracture (about 2–3 cm wide), bordering to a presently open fracture. The wall rock is strongly sericitized.

Quartz, muscovite and fluorite are coarse-grained and the dominating minerals in this sample. Muscovite is coating the fracture and quartz is found in the centre of the fracture. Other minerals (e.g. topaz, Ti-oxide, chalcopyrite, barite, Fe-oxide, Fe-Mg chlorite, sphalerite, sylvite, halite, native gold, and albite) are found in small amounts.

The plateau age defined on the $^{40}\text{Ar}/^{39}\text{Ar}$ step-heating spectrum is $1,424 \pm 2$ Ma (Figure 5-33). It is interpreted as the crystallization age of the muscovite. This age shows that these fillings are related to the intrusion (and/or post-magmatic circulation) of the Götemar granite. The somewhat lower age (minimum ~20 Ma) for the muscovite than for the intrusion of the Götemar granite ($1,452 +11/-9$ Ma, /Åhäll 2001/) might be due to formation of muscovite related to post-magmatic circulation and that the closure temperature for Ar is quite low in muscovite (~350°C).



Figure 5-32. Photograph of the drill core showing a fracture sealed with mainly muscovite, quartz and fluorite.

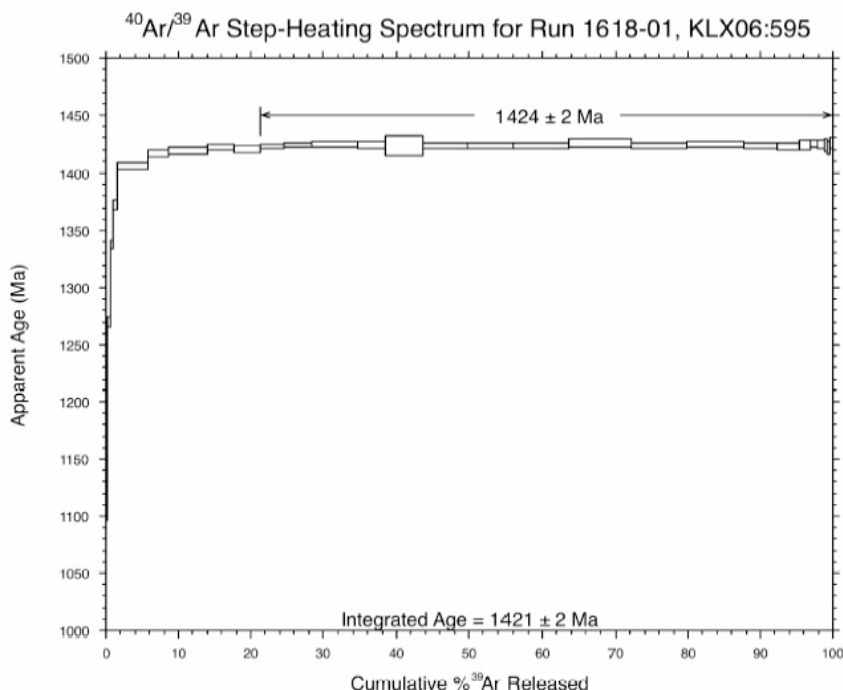


Figure 5-33. $^{40}\text{Ar}/^{39}\text{Ar}$ muscovite step-heating spectrum for sample KLX06: 595.08–595.18 m.

5.13 Sample KLX08: 933.15–933.30 m (hornblende)

The sample shows sealed fractures boarded by red-stained wall rock. Minerals in the fractures are hornblende (most abundant), calcite, titanite (occasionally euhedral), K-feldspar, Fe-Mg chlorite, (magnetite, pyrite, albite and epidote). These minerals are thought to be of generation 3. The sample did not yield a plateau age.



Figure 5-34. Photograph of the drill core showing fractures sealed with mainly hornblende, calcite, K-feldspar and chlorite.

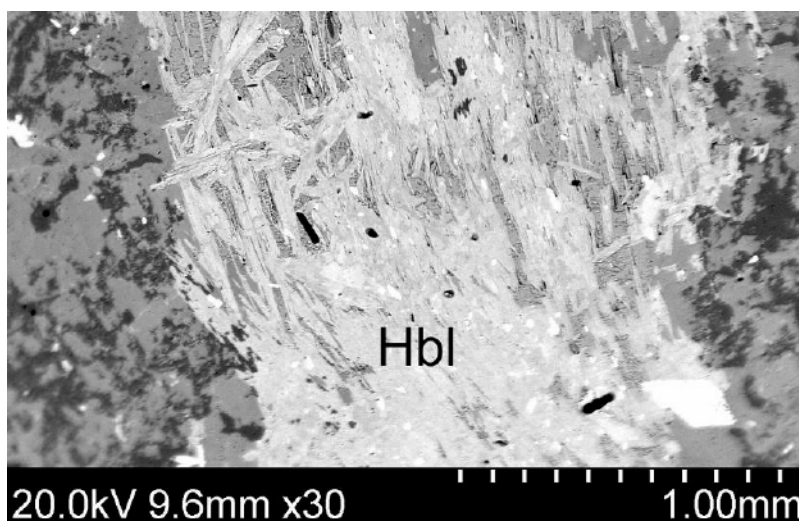


Figure 5-35. Back-scattered SEM-image of hornblende (“Hbl”) and calcite (darker than hornblende) in a sealed fracture.

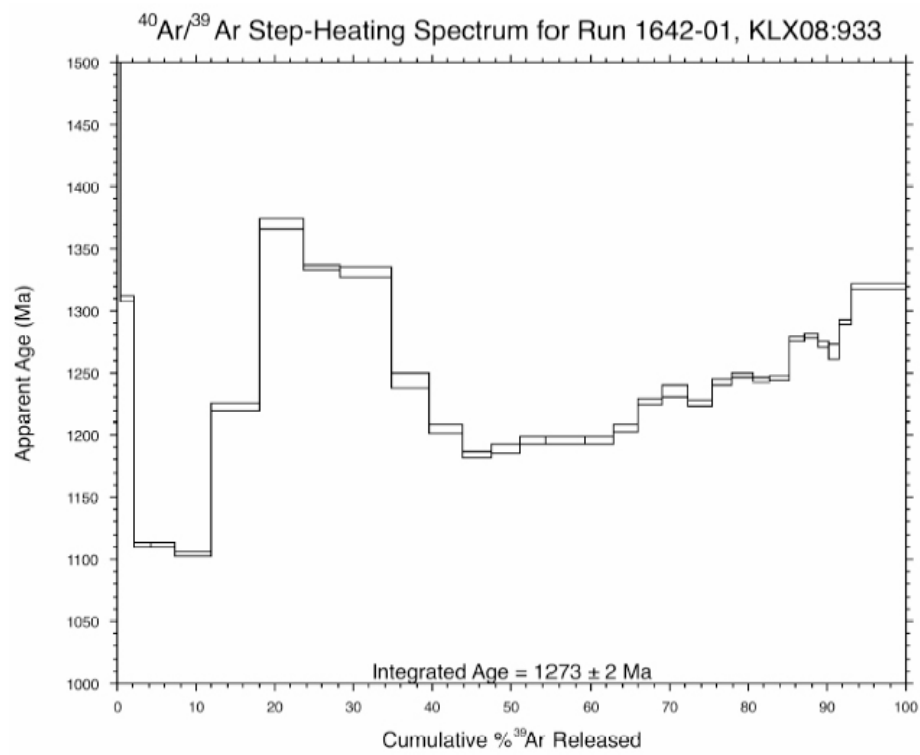


Figure 5-36. ⁴⁰Ar/³⁹Ar hornblende step-heating spectrum for sample KLX08: 933.15–933.30 m.

6 Summary and discussions

The analyses yielded plateau ages for ten samples (Table 6-1). Seven samples yielded ages (adularia and muscovite) in accordance with interpretations from cross-cutting relations, chemistry and isotope studies /Drake and Tullborg 2004, 2005, 2006a,b, 2007/ while two samples yielded younger ages than expected (adularia and muscovite). Four samples did not yield plateau ages or gave insignificant ages (illite, apophyllite and hornblende). Ages were obtained for generation 3, 4 and 6 (Table 6-2). The ages for generation 3 and 4 are also valid for some fillings from generation 5 based on similar wall rock alteration features and stable isotopes. This also provides age constraints for the extensive red-staining of the wall rock in the area.

The mylonites in the area are thought to predate the intrusions of the Götemar and Uthammar granites (~ 1,440–1,450 Ma). The age obtained for muscovite (1,406 Ma) in a mylonite of generation 1 is, thus, not thought to represent the age of the mylonite formation. Instead, the obtained age is thought to represent either re-activation of the mylonites (and formation of muscovite) during the intrusions of the Götemar and Uthammar granites or resetting of the Ar-system in the dated muscovite due to thermal heating of the country rocks during these intrusions. A generation 3 K-feldspar gave a Sveconorwegian age (989 Ma) which is younger than expected. It can either be a generation 3 K-feldspar that has been reset in connection with the Sveconorwegian orogeny or that the K-feldspar was formed during Sveconorwegian reactivation.

Reliable ages were obtained for generation 3 and 4 and for the greisen related fractures in KLX06, which shows that these fracture fillings are related to the intrusion of the Götemar granite (and probably also Uthammar granite). It is also indicated that mylonites were re-activated at this event.

The Palaeozoic generation (6) was also adequately dated (401, 426 and 443–448 Ma for adularia), which is in accordance with earlier datings of this generation in the Götemar granite /Sundblad et al. 2004/. This generation is related in time to the Caledonian orogeny and probably also to its migrating foreland basin.

The results from this study indicate that the bedrock in the area has not been heated to temperatures higher than the blocking temperature for muscovite (~ 350°C) since about 1,400 Ma.

Table 6-1.

Sample	Mineral	Result (Ma) Split 1	Result (Ma) Split 2	Generation /Drake and Tullborg 2007/
KA1755A: 211.70–211.75 m	Muscovite	1,406 ± 3		1
KSH01A: 256.90–257.10 m	Adularia	425.8 ± 1.7		6
KSH03B: 14.97–15.32(l) m	Adularia	443.3 ± 1.2	448.0 ± 1.2	6
KSH03A: 181.93–181.98 m	Adularia	400.9 ± 1.1		6
KSH03A: 186.52–186.62 m	Illite	No plateau		5 or 6
KSH03A: 863.66–863.84 m	Adularia	989 ± 2		3 or later
KLX02: 676.82–677.00 m	Apophyllite	No significant age	No significant age	6
KLX03: 722.72–722.96 m	Muscovite	1,417 ± 3		3 or 4 (wall rock)
KLX03: 970.04–970.07 m	Apophyllite	No plateau	No plateau	6
KLX06: 535.10–535.26 m	Muscovite	1,424 ± 2		Greisen fractures
KLX06: 565.22–565.38 m	Muscovite	1,423 ± 3		Greisen fractures
KLX06: 595.08–595.18 m	Muscovite	1,424 ± 2		Greisen fractures
KLX08: 933.15–933.30 m	Hornblende	No plateau		3

Table 6-2. Schematic fracture filling-sequence from Simpevarp/Laxemar/Äspö with ages from this report. The most abundant minerals in each generation are in bold letters. Minerals in brackets are only found occasionally.

1. Quartz- and epidote-rich mylonite, including muscovite, titanite, Fe-Mg-chlorite, albite, (apatite, calcite and K-feldspar)	}	> 1.45 Ga. Re-activated during intrusion of the Götemar granite
2. Cataclasite		Probably older than 1.45 Ga
a. Early green coloured; epidote -rich, with quartz , Fe-Mg-chlorite , (titanite, K-feldspar, and albite)	}	
b. Late red-brown colour; K-feldspar , chlorite , quartz , hematite , albite, (and illite)		
3. Euhedral quartz , epidote , Fe-Mg chlorite , calcite , pyrite, fluorite, muscovite, (K-feldspar and hornblende)	}	Probably ~ 1.424–1.417 Ga, related to the intrusion of the Götemar granite
4. Prehnite , (fluorite)		
5. a. Calcite , (fluorite and hematite)	}	~ 1.424–0.44 Ga, some fillings (e.g. earliest formed laumontite) is related to the intrusion of the Götemar granite. Some may be Sveconorwegian and some later (possibly Paleozoic)
b. Dark red/brown filling – Adularia, Mg-chlorite, hematite ; sometimes cataclastic.		
c. Calcite, adularia, laumontite, Mg-chlorite, quartz, illite, hematite , (ML-clay – chlorite/illite, albite and apatite)		
6. Calcite, adularia, Fe-chlorite, hematite, fluorite, quartz, pyrite, barite, gypsum, corrensite (and other types of mixed-layer clay), harmotome, REE-carbonate, galena, apophyllite, illite, chalcopyrite, sphalerite, U-silicate, Cu(Zn,Ni,Sn,Fe)-rich minerals, apatite, laumontite (Ti-oxide, Mg-chlorite and albite)	}	~ 0.44–0.40 Ga (Paleozoic)
7. Calcite , pyrite, Fe-oxyhydroxide (near surface)	}	~ 0.40 Ga and later, possibly recent

7 Acknowledgements

SKB is thanked for funding. Sven Åke Larson and Carl-Henric Wahlgren are thanked for providing useful comments. Björn Sandström and Tobias Hermansson are thanked for constructive discussions.

8 References

- Dalrymple G B, Lanphere M A, 1971.** $^{40}\text{Ar}/^{39}\text{Ar}$ technique of K-Ar dating: a comparison with the conventional technique., Earth and Planetary Science Letters, 12, p 300-308.
- Drake H, Tullborg E-L, 2004.** Oskarshamn site investigation. Fracture mineralogy and wall rock alteration, results from drill core KSH01A+B. SKB-P-04-250. 120 pp. Svensk Kärnbränslehantering AB.
- Drake H, Tullborg E-L, 2005.** Oskarshamn site investigation. Fracture mineralogy and wall rock alteration, results from drill cores KAS04, KA1755A and KLX02. SKB-P-05-174. 69 pp. Svensk Kärnbränslehantering AB.
- Drake H, Tullborg E-L, 2006a.** Oskarshamn site investigation. Fracture mineralogy, Results from drill core KSH03A+B. SKB P-06-03. 65 pp. Svensk Kärnbränslehantering AB.
- Drake H, Tullborg E-L, 2006b.** Oskarshamn site investigation. Fracture mineralogy of the Götemar granite, Results from drill cores KKR01, KKR02 and KKR03. SKB P-06-04. 61 pp. Svensk Kärnbränslehantering AB.
- Drake H, Tullborg E-L, 2006c.** Oskarshamn site investigation. Mineralogical, chemical and redox features of red-staining adjacent to fractures, Results from drill cores KSH01A+B and KSH03A+B. SKB P-06-01. 115 pp. Svensk Kärnbränslehantering AB.
- Drake H, Tullborg E-L, 2006d.** Oskarshamn site investigation. Mineralogical, chemical and redox features of red-staining adjacent to fractures, Results from drill core KLX04. SKB P-06-02. 105 pp. Svensk Kärnbränslehantering AB.
- Drake H, Tullborg E-L, 2007.** Oskarshamn site investigation. Fracture mineralogy, Results from drill cores KLX03, KLX04, KLX06, KLX07A, KLX08 and KLX10A. Oskarshamn site investigations. SKB P-06-XX. pp. Svensk Kärnbränslehantering AB (in press).
- Eliasson T, 1993.** Mineralogy, geochemistry and petrophysics of red coloured granite adjacent to fractures. SKB TR-93-06. 68 pp. Svensk Kärnbränslehantering AB.
- McDougall I, Harrison M T, 1999.** Geochronology and Thermochronology by the $^{40}\text{Ar}/^{39}\text{Ar}$ Method, Second edition. Oxford University Press. Oxford, 269 pp.
- Nisca D H, 1987.** Aerogeophysical interpretation: bedrock and tectonic analysis. SKB PR-25-87-04. pp. Svensk Kärnbränslehantering AB.
- Renne P R, Swisher C C, Deino A L, Karner D B, Owena T L, DePaolo D J, 1998.** Intercalibration of standards, absolute ages and uncertainties in $^{40}\text{Ar}/^{39}\text{Ar}$ dating., Chemical Geology, 145, p. 117–152.
- Sundblad K, Alm E, Huhma H, Vaasjoki M, Sollien D B, 2004.** Early Devonian tectonic and hydrothermal activity in the Fennoscandian Shield; evidence from calcite-fluorite-galena mineralization, In: Mertanen S (ed), Extended abstracts, 5th Nordic Paleomagnetic workshop. -Supercontinents, remagnetizations and geomagnetic modelling., Geological Survey of Finland, p 67–71.
- Talbot C, Riad L, 1988.** Natural fractures in the Simpevarp area. PR-25-87-03. 28 pp. Svensk Kärnbränslehantering AB.
- Åhäll K-I, 2001.** Åldersbestämning av svårdaterade bergarter i sydöstra Sverige. SKB R-01-60. 28 pp. Svensk Kärnbränslehantering AB.

Appendix 1

$^{40}\text{Ar}/^{39}\text{Ar}$ -data

KLX06:595, Run ID# 1618-01 (J = 0.01066 ± 0.000012):							MUSCOVITE				% $^{40}\text{Ar}/^{39}\text{Ar}$			Age (Ma)		\pm Age	
Run ID	Pwr/T°C	Ca/K	$^{38}\text{Ar}/^{39}\text{Ar}$	% $^{38}\text{Ar}(\text{Ca})$	$^{40}\text{Ar}/^{39}\text{Ar}$	Mol ^{39}Ar	% Step	Cum. %	% $^{40}\text{Ar}^*$	Age (Ma)	\pm Age						
1618-01A	1.8	0.08949	0.057776	0	62.00294	4.4806E+11	0.1	0.1	78.4	915.37176	5.23325						
1618-01B	2	0.01761	0.034545	0	79.13738	6.646E+11	0.1	0.2	88.6	1,103.59479	3.62899						
1618-01C	2.3	-0.01323	0.040889	0	95.8668	2.4803E+12	0.4	0.5	88.8	1,270.1741	2.30473						
1618-01D	2.5	0.01452	0.00537	0	103.10383	2.9198E+12	0.4	1	98.5	1,337.72755	1.83288						
1618-01E	2.7	0.00115	0.001846	0	106.90144	4.1536E+12	0.6	1.6	99.5	1,372.18937	2.13795						
1618-01F	3	0.00446	0.001563	0	110.71587	2.7917E+13	4.1	5.7	99.6	1,406.15354	1.34215						
1618-01G	3.2	0.00439	0.000587	0.1	111.88647	2.0176E+13	3	8.7	99.8	1,416.4498	1.55597						
1618-01H	3.4	0.00341	0.000688	0.1	112.12115	3.594E+13	5.3	14	99.8	1,418.50692	1.47473						
1618-01I	3.6	0.00019	0.00006	0	112.52874	2.5329E+13	3.7	17.7	100	1,422.07414	1.14177						
1618-01J	3.8	0.00021	0.000056	0.1	112.30462	2.488E+13	3.7	21.4	100	1,420.11354	1.43412						
1618-01K	*4.0	0.00195	0.000172	0.2	112.57627	2.208E+13	3.3	24.6	100	1,422.48962	0.88614						
1618-01L	*4.2	0.00301	0.00012	0.3	112.76781	2.6374E+13	3.9	28.5	100	1,424.1632	0.95383						
1618-01M	*4.4	0.00492	0.000234	0.3	112.85846	4.1053E+13	6.1	34.6	99.9	1,424.95468	1.20233						
1618-01N	*4.6	0.00546	0.000285	0.3	112.70039	2.6336E+13	3.9	38.5	99.9	1,423.5743	1.4322						
1618-01O	*4.8	0.00524	0.000262	0.3	112.7007	3.4996E+13	5.2	43.6	99.9	1,423.57697	4.21857						
1618-01P	*5.0	0.00373	0.000148	0.3	112.68171	4.1821E+13	6.2	49.8	100	1,423.41113	1.37258						
1618-01Q	*5.2	0.00352	0.000093	0.5	112.65768	4.2263E+13	6.2	56	100	1,423.2011	1.3056						
1618-01R	*5.4	0.003	0.000107	0.4	112.61616	5.1313E+13	7.6	63.6	100	1,422.83835	1.25368						
1618-01S	*5.6	0.00128	0.000106	0.2	112.9645	5.8079E+13	8.6	72.2	100	1,425.88015	1.92912						
1618-01T	*5.8	0.00198	0.000112	0.2	112.68531	5.1307E+13	7.6	79.8	100	1,423.44226	1.22168						
1618-01U	*6.0	0.00127	0.000097	0.2	112.78614	5.4354E+13	8	87.8	100	1,424.32329	1.04171						
1618-01V	*6.2	0.00272	0.000137	0.3	112.67867	3.0969E+13	4.6	92.3	100	1,423.38453	1.11178						
1618-01W	*6.4	0.00104	0.000195	0.1	112.59691	2.0473E+13	3	95.4	99.9	1,422.67005	1.77292						
1618-01X	*6.7	0.00104	0.000215	0.1	112.73954	1.1142E+13	1.6	97	99.9	1,423.91625	2.0897						
1618-01Y	*7.0	0.00437	0.000196	0.3	112.8355	6.3191E+12	0.9	97.9	99.9	1,424.75428	1.53226						
1618-01Z	*7.4	0.00087	0.000165	0.1	112.81359	5.5453E+12	0.8	98.8	100	1,424.56297	1.7367						
1618-01ZA	*7.8	0.00002	0.000057	0	112.72177	2.965E+12	0.4	99.2	100	1,423.76111	2.73075						
1618-01ZB	*8.5	0.00222	0.001094	0	112.50588	2.1847E+12	0.3	99.5	99.7	1,421.87426	2.73736						
1618-01ZC	*10.0	0.00151	0.000606	0	112.92626	3.223E+12	0.5	100	99.8	1,425.54645	2.19305						
Integ. Age =												1,421	2				
(•) Plateau Age =												1,424	2				

KLX06:535, Run ID# 1619-01 (J = 0.01066 ± 0.0000012):												
Run ID	Pwrt/T°C	Ca/K	% ³⁶ Ar/ ³⁹ Ar	% ³⁶ Ar(Ca)	⁴⁰ Ar/ ³⁹ Ar	Muscovite	Mol ³⁹ Ar	% Step	Cum. %	% ⁴⁰ Ar*	Age (Ma)	± Age
1619-01A	2.7	0.00096	0.026689	0	109.07185	5.0789E+12	0.8	0.8	93.3	1,391.59329	2.0065	
1619-01B	3.1	0.0067	0.008321	0	111.89586	9.5901E+12	1.5	2.3	97.9	1,416.53218	1.42033	
1619-01C	3.3	0.00508	0.001573	0	112.39652	1.4394E+13	2.3	4.6	99.6	1,420.91772	1.19957	
1619-01D	*3.5	0.00504	0.00116	0.1	112.61677	2.9589E+13	4.6	9.2	99.7	1,422.8436	1.34588	
1619-01E	*3.7	0.00863	0.000852	0.1	112.57448	3.1866E+13	5	14.2	99.8	1,422.474	1.74964	
1619-01F	*3.9	0.0043	0.000711	0.1	112.77655	6.2455E+13	9.8	24	99.8	1,424.23952	1.81055	
1619-01G	*4.1	0.00888	0.000557	0.2	112.51682	4.3134E+13	6.8	30.7	99.9	1,421.9699	2.39795	
1619-01H	*4.3	0.00823	0.000205	0.6	112.87385	8.4815E+13	13.3	44	99.9	1,425.08902	1.44044	
1619-01I	*4.5	0.00365	0.000184	0.3	112.61496	7.2373E+13	11.3	55.4	100	1,422.82781	1.37004	
1619-01J	*4.7	0.00843	0.000336	0.3	112.6023	4.5301E+13	7.1	62.5	99.9	1,422.71718	1.5894	
1619-01K	*4.9	0.00686	0.000204	0.5	112.65815	4.4404E+13	7	69.4	99.9	1,423.20528	3.34401	
1619-01L	*5.1	0.00648	0.000175	0.5	112.73642	3.3763E+13	5.3	74.7	100	1,423.88906	1.4424	
1619-01M	*5.3	0.00876	0.000211	0.6	112.59609	3.0149E+13	4.7	79.4	99.9	1,422.66292	1.00578	
1619-01N	*5.5	0.00562	0.000046	1.7	112.71437	1.971E+13	3.1	82.5	100	1,423.69644	1.14273	
1619-01O	*5.7	0.00431	0.000117	0.5	112.83362	2.188E+13	3.4	85.9	100	1,424.73781	1.30069	
1619-01P	*5.9	0.0086	0.000146	0.8	112.66408	1.713E+13	2.7	88.6	100	1,423.25706	1.15486	
1619-01Q	*6.1	0.0111	0.000204	0.7	112.82787	1.8333E+13	2.9	91.5	99.9	1,424.6876	1.43176	
1619-01R	*6.3	0.00659	0.000068	1.3	112.73752	8.6527E+12	1.4	92.9	100	1,423.89862	1.82163	
1619-01S	*6.5	0.02267	0.000054	5.8	112.70909	8.5277E+12	1.3	94.2	100	1,423.65029	2.11243	
1619-01T	*6.7	0.03489	0.000403	1.2	112.74239	7.5953E+12	1.2	95.4	99.9	1,423.94114	1.58501	
1619-01U	*7.0	0.04551	0.000031	20	112.76893	7.423E+12	1.2	96.5	100	1,424.17298	1.50442	
1619-01V	*7.5	0.04	0.000243	2.3	112.85379	6.4448E+12	1	97.6	99.9	1,424.91388	1.58007	
1619-01W	*10.0	0.0271	0.00021	1.8	112.68361	1.5583E+13	2.4	100	99.9	1,423.42773	1.07836	
Integ. Age =										1,423	3	
(•) Plateau Age =										1,424	2	
										95.4		

KLX03:970, Run ID# 1620-01 (J = 0.01066 ± 0.0000012):						
Run ID	Pwr/T°C	Ca/K	% ³⁶ Ar/ ³⁹ Ar	Apophyllite % ³⁶ Ar(Ca)	Mol ³⁹ Ar	% Step
1620-01A	2.4	3.90791	0.000688	78.2	1.67648	2.6129E+13
1620-01B	2.7	3.98817	0.000578	95.1	2.35636	5.1156E+13
1620-01C	2.9	4.10068	0.046024	1.2	1.69686	3.8321E+12
1620-01D	5	4.01749	0.000708	78.1	2.3966	2.4717E+13
Integ. Age =						41.3
						0.4

KLX03:970, Run ID# 1620-02 (J = 0.01066 ± 0.0000012):						
Run ID	Pwr/T°C	Ca/K	% ³⁶ Ar/ ³⁹ Ar	Apophyllite % ³⁶ Ar(Ca)	Mol ³⁹ Ar	% Step
1620-02A	2	3.96307	0.002464	22.2	2.82313	5.3583E+12
1620-02B	2.2	3.99405	0.000927	59.3	2.49183	4.7396E+13
1620-02C	2.3	4.15872	0.000801	71.5	1.85858	7.1494E+13
1620-02D	2.4	4.58506	0.000946	66.7	1.58531	5.8579E+13
1620-02E	2.5	35.38421	0.005116	95.3	2.68972	2.3733E+12
Integ. Age =						1.3
						100
						97.4
						37.54
						0.18

KSH03:863, Run ID# 1621-01 (J = 0.01066 ± 0.000012); Pwr/T°C Ca/K % ³⁶ Ar/ ³⁹ Ar							Kspar % Ar/ ³⁹ Ar			
Run ID	Pwr/T°C	Ca/K	% ³⁶ Ar(Ca)	Mol ³⁸ Ar	% Step	Cum. %	% ⁴⁰ Ar*	Age (Ma)	± Age	
1621-01A	2.2	0.02242	0.01342	0	117.67322	1.7796E+13	3.2	96.7	1,466.50245	2.6781
1621-01B	2.4	0.00037	0.000009	0.6	52.9192	1.369E+13	2.5	5.7	100	807.0044
1621-01C	2.6	0.00065	0.000004	2.4	55.9369	9.9667E+12	1.8	7.5	100	843.73178
1621-01D	2.8	0.00447	0.000108	0.6	57.63724	1.4277E+13	2.6	10.1	99.9	864.10139
1621-01E	3	0.01113	0.000015	10.4	59.0577	1.4661E+13	2.7	12.7	100	880.94351
1621-01F	3.2	0.01859	0.0001	2.5	60.71157	9.5634E+12	1.7	14.5	100	900.35721
1621-01G	3.4	0.03366	0.000081	5.7	62.05837	1.0918E+13	2	16.4	100	916.01334
1621-01H	3.6	0.07394	0.000572	1.8	63.82881	1.2047E+13	2.2	18.6	99.7	936.38975
1621-01I	3.8	0.12002	0.000614	2.7	65.54213	1.2668E+13	2.3	20.9	99.7	955.89205
1621-01J	4	0.12254	0.000594	2.8	65.71677	1.1496E+13	2.1	23	99.7	957.86807
1621-01K	4.2	0.0985	0.00004	34.2	65.62971	1.1386E+13	2.1	25	100	956.88331
1621-01M	4.6	0.0381	0.000067	7.8	66.01412	1.1311E+13	2	27.1	100	961.22768
1621-01N	4.8	0.04062	0.000674	0.8	66.66445	9.6518E+12	1.7	28.8	99.7	968.55378
1621-01O	5	0.05516	0.000522	1.5	66.43607	1.1049E+13	2	30.8	99.8	965.98442
1621-01Q	5.4	0.0526	0.000086	8.4	66.57083	1.1641E+13	2.1	32.9	100	967.50093
1621-01R	5.6	0.05564	0.000286	2.7	66.50175	1.3637E+13	2.5	35.4	99.9	966.72369
1621-01S	5.8	0.03294	0.000268	1.7	66.84993	1.0864E+13	2	37.3	99.9	970.63776
1621-01T	6	0.05299	0.000535	1.4	67.09683	1.6994E+13	3.1	40.4	99.8	973.40814
1621-01U	•6.3	0.04034	0.000663	0.8	68.49453	2.594E+13	4.7	45.1	99.7	989.01147
1621-01V	•6.8	0.02008	0.00094	0.3	68.37629	1.1547E+14	20.9	66	99.6	987.69679
1621-01W	•7.5	0.01103	0.001158	0.1	68.72901	1.4152E+14	25.6	91.6	99.5	991.61597
1621-01X	•9.0	0.0022	0.001288	0	68.44546	4.6688E+13	8.4	100	99.4	988.46604
Integ. Age =								985	2	
(•) Plateau Age =								989	2	

KSH03:186, Run ID# 1622-01 (J = 0.01066 ± 0.000012):						
Run ID	Pwr/T/C	Ca/K	$^{36}\text{Ar}/^{39}\text{Ar}$	% $^{36}\text{Ar}(\text{Ca})$	Mol ^{39}Ar	% Step
1622-01A	1.8	0.08003	0.008322	0.1	9.02948	2.2
1622-01B	2	0.06449	0.004165	0.2	16.82088	2.1
1622-01C	2.2	0.06978	0.002956	0.3	24.56706	2.0287E+13
1622-01E	2.6	0.05924	0.001363	0.6	30.45401	5.7049E+13
1622-01F	2.8	0.05065	0.001001	0.7	31.20208	6.7723E+13
1622-01G	3.4	0.05061	0.000418	1.7	32.69732	8.4314E+13
1622-01H	3.6	0.04625	0.000256	2.5	31.6098	4.7879E+13
1622-01I	3.9	0.05245	0.000449	1.6	29.0569	1.9815E+13
1622-01J	4.4	0.04911	0.000512	1.3	29.58089	1.7555E+13
1622-01K	4.8	0.06724	0.000465	2	28.88911	1.5703E+13
1622-01L	5.2	0.16177	0.00043	5.2	28.62195	1.5466E+13
1622-01M	5.6	0.2136	0.000581	5.1	28.58556	1.4758E+13
1622-01N	6.5	0.26485	0.000453	8.1	28.1326	2.183E+13
1622-01O	9	0.1647	0.000401	5.7	27.48569	2.7622E+13
1622-01P	12	0.3082	0.000353	12	26.58513	4.31E+13
Integ. Age =						
					488.5	1.1

KSH01:257, Run ID# 1640-01 (J = 0.01066 ± 0.000012):						
Run ID	Pwr/T/C	Ca/K	$^{36}\text{Ar}/^{39}\text{Ar}$	% $^{36}\text{Ar}(\text{Ca})$	Kspar $^{40}\text{Ar}/^{39}\text{Ar}$	Mol ^{39}Ar
1640-01A	2.2	0.06037	0.001292	0.6	22.20261	1.0398E+14
1640-01B	2.6	0.03303	0.000406	1.1	23.55502	6.9765E+13
1640-01D	•3.4	0.01737	0.000125	1.9	25.01283	1.986E+14
1640-01E	•3.8	0.02504	0.000136	2.5	25.02787	1.4077E+14
1640-01F	•4.2	0.02279	0.000179	1.8	24.78663	1.1383E+14
1640-01G	7	0.00776	0.000209	0.5	25.7814	3.1496E+13
Integ. Age =						
					68	425.8
(•) Plateau Age =						
						1.7

KLX03:722, Run ID# 1641-01 (J = 0.01066 ± 0.0000012):						
Run ID	Pwr/T°C	Ca/K	% ³⁶ Ar/ ³⁹ Ar	% ³⁶ Ar(Ca)	⁴⁰ Ar/ ³⁹ Ar	Musc/Sericite
1641-01A	1.5	0.7758	0.023582	0.5	86.45681	3.7343E+11
1641-01B	1.7	1.62253	0.007795	2.9	100.91216	1.411E+12
1641-01C	1.9	0.16264	0.001238	1.8	110.30421	9.1525E+12
1641-01D	•2.1	0.05327	0.000819	0.9	111.89373	2.1621E+13
1641-01E	•2.3	0.04095	0.000354	1.6	112.00941	4.1838E+13
1641-01F	2.5	0.04188	0.000021	27.9	110.33549	1.0421E+13
1641-01G	2.7	0.16215	0.000803	2.8	110.45244	6.0325E+12
1641-01H	2.9	0.14657	0.000687	2.9	106.66049	2.3394E+12
1641-01I	3.2	0.33463	0.001115	4.1	105.71808	6.0271E+12
Integ. Age =				64	6.1	100
(•) Plateau Age =				99.7	99.8	99.7
				1,407	3	1,407
				1,417	3	1,417

KLX06:565, Run ID# 1643-01 (J = 0.01066 ± 0.0000012):						
Run ID	Pwr/T°C	Ca/K	% ³⁶ Ar/ ³⁹ Ar	% ³⁶ Ar(Ca)	⁴⁰ Ar/ ³⁹ Ar	Muscovite
1643-01A	•2.3	0.00744	0.006624	0	112.60289	4.9418E+13
1643-01B	•2.6	0.00955	0.000595	0.2	112.70706	4.1842E+13
1643-01C	•0.0	0.01043	0.000662	0.2	112.53413	2.387E+13
1643-01E	•3.3	0.28856	0.006368	0.6	113.18417	9.5024E+11
1643-01F	•6.0	0.07208	0.001424	0.7	112.38337	7.1995E+12
Integ. Age =				5.8	100	99.6
(•) Plateau Age =				100	99.6	99.6
				1,423	3	1,423
				1,423	3	1,423

KLX08-933, Run ID# 1642-01 (J = 0.01066 ± 0.000012);											
Run ID	Pwr/T°C	Ca/K	% ³⁶ Ar/ ³⁹ Ar	% ³⁶ Ar(Ca)	Hornblende	Mol ³⁹ Ar	% Step	Cum. %	% ⁴⁰ Ar*	Age (Ma)	± Age
1642-01A	1.5	1.89616	1.203062	0	2,440.0608	6.8589E+11	0.1	0.1	87.3	5,946.68225	7.73308
1642-01B	1.7	1.6599	0.140606	0.2	404.77883	2.4731E+12	0.3	0.4	90.7	3,013.75095	3.26136
1642-01C	1.9	5.82072	0.014417	5.6	100.04174	1.3258E+13	1.8	2.2	96.1	1,309.45284	1.35544
1642-01D	2.1	9.74285	0.012547	10.7	79.88613	1.5467E+13	2	4.2	96	1,111.38848	1.10678
1642-01E	2.3	11.17629	0.008443	18.2	79.87393	2.3357E+13	3.1	7.3	97.5	1,111.26175	0.9303
1642-01F	2.5	10.89891	0.003737	40.2	79.17673	3.4238E+13	4.5	11.9	99.2	1,104.0053	1.0662
1642-01G	2.7	5.0549	0.009839	7.1	90.88949	4.6374E+13	6.1	18	97.1	1,222.20069	1.60575
1642-01H	2.8	8.62112	0.008564	13.9	106.70025	4.2802E+13	5.7	23.7	98	1,370.38008	2.04169
1642-01I	2.9	9.97858	0.005794	23.7	102.76223	3.4624E+13	4.6	28.3	98.7	1,334.59523	1.13139
1642-01J	3	11.66064	0.006013	26.7	102.35813	4.9262E+13	6.5	34.8	98.7	1,330.88269	1.9654
1642-01K	3.1	7.47928	0.002886	35.7	93.08866	3.658E+13	4.8	39.6	99.4	1,243.55464	3.00886
1642-01L	3.2	6.04159	0.002692	30.9	89.13251	3.2539E+13	4.3	43.9	99.4	1,204.95686	1.91901
1642-01M	3.3	4.71941	0.001457	44.6	87.02157	2.7319E+13	3.6	47.6	99.7	1,184.01876	1.04661
1642-01N	3.4	4.17684	0.001428	40.3	87.52272	2.6755E+13	3.5	51.1	99.7	1,189.01164	1.80267
1642-01O	3.5	3.65409	0.00132	38.1	88.21836	2.5333E+13	3.4	54.5	99.7	1,195.91935	1.3333
1642-01P	3.6	3.76152	0.001351	38.4	88.21239	3.5744E+13	4.7	59.2	99.7	1,195.86017	1.48422
1642-01Q	3.7	2.60989	0.000975	36.9	88.14718	2.7907E+13	3.7	62.9	99.8	1,195.21373	1.54179
1642-01R	3.8	2.73676	0.001145	32.9	89.17022	2.2824E+13	3	65.9	99.7	1,205.32868	1.37047
1642-01S	3.9	2.47939	0.000863	39.6	91.35424	2.3195E+13	3.1	69	99.8	1,226.73456	1.34798
1642-01T	4.1	2.85679	0.001198	32.9	92.26678	2.5494E+13	3.4	72.4	99.7	1,235.60379	2.43252
1642-01U	4.3	3.12974	0.001211	35.6	91.2769	2.2369E+13	3	75.3	99.7	1,225.98083	1.24129
1642-01V	4.5	2.97639	0.001109	37	93.05674	1.8861E+13	2.5	77.8	99.8	1,243.2465	1.23394
1642-01W	4.7	3.12928	0.001227	35.1	93.57912	2.1405E+13	2.8	80.7	99.7	1,248.28277	0.84397
1642-01X	4.9	2.98962	0.001108	37.2	93.18654	1.5374E+13	2	82.7	99.8	1,244.49923	0.94979
1642-01Y	5.1	2.54974	0.00085	41.3	93.33045	1.8535E+13	2.5	85.2	99.8	1,245.88713	0.96349
1642-01Z	5.3	5.63982	0.00193	40.3	96.61218	1.4748E+13	2	87.1	99.6	1,277.24975	1.0867
1642-01AA	5.5	3.80904	0.00113	46.4	96.86355	1.3815E+13	1.8	88.9	99.8	1,279.62969	0.99708
1642-01AB	5.7	3.43846	0.00099	47.9	96.22401	8.7607E+12	1.2	90.1	99.8	1,273.56849	1.30679
1642-01AC	6	2.35066	0.000843	38.4	95.57024	1.044E+13	1.4	91.5	99.8	1,267.35115	2.98555
1642-01AD	7	2.90097	0.001012	39.5	98.05727	1.1822E+13	1.6	93	99.8	1,290.88912	1.13554
1642-01AE	10	4.75	0.001384	47.3	101.128	5.2486E+13	7	100	99.8	1,319.53395	1.24532
Integ. Age =										1.273	2

KLX02:676, Run ID# 1644-01 (J = 0.01066 ± 0.000012);										
Run ID	Pwr/T°C	Ca/K	% ³⁶ Ar/ ³⁹ Ar	Apophyllite 40*Ar/ ³⁹ Ar(Ca)	Mol 39Ar	% Step	Cum. %	% ⁴⁰ Ar*	Age (Ma)	± Age
1644-01A	1.7	4.53645	0.001316	47.5	2.14167	4.0654E+13	5.5	91.3	40.72427	0.189
1644-01B	•1.9	4.24368	0.000933	62.7	0.61572	3.3421E+14	45.4	50.9	85.6	11.80248
1644-01C	•2.1	0.53063	0.000796	9.2	0.53179	1.0058E+14	13.7	64.6	71.3	0.16006
1644-01D	•2.3	4.20028	0.000799	72.4	0.63575	1.507E+14	20.5	85.1	90.7	12.18521
1644-01E	•2.5	4.17913	0.000799	72	0.54163	1.0989E+14	14.9	100	89.1	10.38646
Integ. Age =	(•) Plateau Age =								13.06	0.09
				94.5					11.6	0.8

KLX02:676, Run ID# 1644-02 (J = 0.01066 ± 0.000012);										
Run ID	Pwr/T°C	Ca/K	% ³⁶ Ar/ ³⁹ Ar	Apophyllite 40*Ar/ ³⁹ Ar(Ca)	Mol 39Ar	% Step	Cum. %	% ⁴⁰ Ar*	Age (Ma)	± Age
1644-02A	1.7	4.16591	0.001728	33.2	2.41163	2.7828E+13	2.3	2.3	87.6	45.7931
1644-02B	•1.9	4.17821	0.000853	67.5	0.95383	1.6157E+14	13.4	15.7	92.1	18.25099
1644-02C	•2.1	4.14771	0.000856	66.7	0.96908	3.9692E+14	32.9	48.6	92	18.5412
1644-02D	•2.3	4.21927	0.000985	59	1.14318	1.054E+14	8.7	57.3	90.5	21.85219
1644-02E	•2.5	4.15868	0.000803	71.4	0.96326	4.4412E+14	36.8	94.1	93.4	18.43036
1644-02F	•2.7	4.19274	0.000514	112.3	1.08466	1.4426E+13	1.2	95.3	101.7	20.73989
1644-02G	•2.9	4.14708	0.000698	81.8	1.14123	5.729E+13	4.7	100	96.8	21.81507
Integ. Age =	(•) Plateau Age =								19.56	0.08
				97.7					18.9	1